



# CATÓLICA

## ESCOLA SUPERIOR DE BIOTECNOLOGIA

---

PORTO

**CHARACTERIZATION OF TWO *QUERCUS SUBER* L. AQUAPORINS UPON  
HETEROLOGOUS EXPRESSION IN YEAST. TRANSPORT ACTIVITY AND REGULATION**

by

Raquel Antunes Quaresma

November 2018



# CATÓLICA

## ESCOLA SUPERIOR DE BIOTECNOLOGIA

---

PORTO

### **CHARACTERIZATION OF TWO *QUERCUS SUBER* L. AQUAPORINS UPON HETEROLOGOUS EXPRESSION IN YEAST. TRANSPORT ACTIVITY AND REGULATION**

Thesis presented to *Escola Superior de Biotecnologia* of the *Universidade Católica Portuguesa*  
to fulfill the requirements of Master of Science degree in Applied Microbiology

by

Raquel Antunes Quaresma

Place: Laboratório de Bioenergética Microbiana – Instituto Superior de Agronomia,  
Universidade de Lisboa

Supervision: Farzana Sabir and Catarina Prista

November 2018

## Resumo

*Quercus suber* L. (sobreiro) é um importante recurso florestal natural com relevância ecológica (sequestro de carbono, ciclo da água, reservatório de biodiversidade, proteção do solo) e impacto socioeconómico em Portugal. Compreender as causas do declínio do sobreiro e obter um conhecimento molecular mais profundo dos transportadores que intervêm nos processos que lidam com as respostas do ecossistema a fatores externos, emergiu como uma questão importante a abordar.

As aquaporinas desempenham, provavelmente, um papel importante na forma como esta espécie lida com o stresse hídrico. A análise genómica revelou a presença de vários genes putativos de aquaporinas, mas o estudo do papel fisiológico de cada aquaporina é frequentemente impossibilitado pela sua expressão a nível tecidual.

Assim, este estudo visou a caracterização molecular e fisiológica de duas aquaporinas de *Quercus suber* L., analisando também a sua regulação.

Para esse efeito, selecionaram-se dois genes que codificam aquaporinas, que foram clonados e expressos numa estirpe *aqy-null* de *Saccharomyces cerevisiae*, a fim de se caracterizar individualmente cada uma das aquaporinas (QsTIP2;1 e QsPIP2;4) em relação ao transporte de água e de substratos atípicos.

A caracterização funcional destas aquaporinas permitiu verificar que ambas as aquaporinas são funcionais como transportadores de água e de substratos atípicos, nomeadamente peróxido de hidrogénio e boro, sendo o resíduo Thr<sup>70</sup> da aquaporina QsPIP2;4 determinante para o seu funcionamento enquanto transportador de água. Em relação aos aspectos relacionados com a regulação do transporte de água, verificou-se que nenhuma das aquaporinas estudadas é regulada por fosforilação mas são ambas reguladas pelo pH extracelular, sendo a sua atividade maior a pH 6.8. Para além disso, e contrariamente ao esperado, a atividade de QsPIP2;4 A aumenta em presença de cloreto de mercúrio 54%. Este aumento é revertido pela adição de  $\beta$ -mercaptoethanol em 14%.

**Palavras-chave:** Aquaporinas, levedura, regulação, sobreiro, transporte de água e substratos atípicos.

## Abstract

*Quercus suber* L. (cork oak) is an important natural forest resource with ecological relevance (carbon sequestration, water cycle, biodiversity reservoir, soil protection) and socioeconomic impact in Portugal. Understanding the causes of cork oak decline and gaining deeper molecular knowledge of transporters involved in processes that deal with ecosystem responses to external factors, has emerged as an important issue to be addressed.

Aquaporins probably play an important role in how this species copes with water stress. Genomic analysis has revealed several putative aquaporin-genes, but the study of the physiological role of each aquaporin is often difficult due to its tissue level expression.

The present study aimed to perform the molecular and physiological characterization of two *Quercus suber* L. aquaporins, as well as to study their regulation.

For this purpose, two genes encoding aquaporins were selected, which were cloned and expressed in a *Saccharomyces cerevisiae* aqy-null strain, in order to characterize individually each of the aquaporins (QsTIP2;1 and QsPIP2;4) in relation to transport water and atypical substrates.

The functional characterization of these aquaporins allowed us to verify that both aquaporins are functional as water channels and transport of atypical substrates, namely hydrogen peroxide and boron. The Thr<sup>70</sup>residue of aquaporin QsPIP2;4 was considered determinant for its functioning as a water transporter. Regarding the aspects related to the regulation of water transport, it was verified that none of the studied aquaporins are regulated by phosphorylation but are both regulated by extracellular pH, and their activity is higher at pH 6.8. In addition, contrary to what was expected, the activity of QsPIP2;4 A increases in the presence of mercury chloride by 54%. This increase is reversed by the addition of  $\beta$ -mercaptoethanol by 14%.

**Keywords:** Aquaporins, cork oak, regulation, transport of water and atypical substrates, yeast,

## Agradecimentos

No final deste percurso não posso deixar de tecer alguns agradecimentos.

Em primeiro lugar, quero agradecer à professora Maria Conceição Loureiro Dias por ter permitido o desenvolvimento deste projeto no seu laboratório.

À professora Catarina Prista, o meu mais sincero obrigada por tudo o que fez por mim. Agradeço de coração não me ter deixado cair quando seria muito mais fácil dizer que não. Obrigada por ter salvado o meu ano, a minha tese, o meu mestrado. Nenhuma palavra será alguma vez suficiente para exprimir o meu agradecimento.

À Farzana, um enorme obrigada por tudo o que me ensinou. Um obrigada por todos os momentos divertidos que tivemos juntas, por todas as vezes em que me consolou e por todas as palavras de força.

Agradeço à professora Leonor Morais e à Vera Inácio, por terem fornecido os cDNAs de sobreiro que permitiram o desenvolvimento deste projeto.

A todos os meus colegas que estiveram ou que ainda estão a desenvolver os seus projetos de investigação no Laboratório de Bioenergética Microbiana, agradeço todos os momentos. Desde a fantástica receção, às limpezas em conjunto, às arrumações e à entreaajuda.

Agradeço a todas as pessoas que se cruzaram comigo neste último ano a nível profissional pois sem vós nada disto seria possível.

À minha família, em particular aos meus pais, quero deixar um especial agradecimento por lutarem todos os dias pela minha formação académica, pela minha realização profissional mas também pessoal.

Aos meus mais caros amigos, um grande obrigada por todo o apoio. Obrigada por tentarem sempre acompanhar as minhas conversas científicas. Obrigada por todas as vezes em que as aquaporinas foram aquapurporinas, por todos os momentos divertidos, por estarem sempre presentes e principalmente por todos os “eu não percebo nada disso mas quero ir ver-te”.

Ao Pedro, que me apoiou incondicionalmente em todas as minhas escolhas, que me apoiou em todos os maus momentos e que festejou comigo todas as vitórias. Agradeço toda a companhia que me fez, todas as gargalhadas que me roubou e todos os momentos em que insistiu para que eu continuasse.

# Contents

Resumo .....	i
Abstract .....	ii
Agradecimientos .....	iii
Contents .....	iv
List of figures .....	vi
List of tables.....	ix
1. Introduction.....	1
1.1 <i>Quercus suber</i> L.....	1
1.2 Aquaporins .....	3
1.2.1 Structure of aquaporins.....	3
1.2.2 Water transport in plants.....	5
1.2.3 Aquaporins from plants .....	5
1.2.4 Physiological role of aquaporins in the transport of unconventional solutes and resistance to abiotic stresses .....	7
1.2.5 Regulation .....	7
1.3 <i>Saccharomyces cerevisiae</i> .....	9
1.4 Aims .....	11
2. Materials and Methods.....	12
2.1 Biological Material .....	12
2.2 Cloning and heterologous expression of <i>Q. suber</i> aquaporins in <i>Saccharomyces cerevisiae</i> .....	12
2.4 Sequence analysis .....	14
2.5 Water transport assays of <i>Q. suber</i> aquaporins expressed in <i>S. cerevisiae</i> .....	15
2.6 Growth assays under osmotic stress and sensitivity tests on atypical substrates - Drop-tests .....	15
2.7 Statistical analysis .....	16
3. Results .....	17
3.1 Cloning, sequence analysis and heterologous expression of <i>Q. suber</i> L. aquaporins in <i>aqy-null S. cerevisiae</i> .....	17
3.1.1 PCR and cloning.....	17
3.1.2 Insert analysis.....	17
3.1.3 Heterologous expression in <i>aqy-null Saccharomyces cerevisiae</i> .....	19
3.1.4 Sequence analysis.....	20
3.1.5 Topology prediction.....	21
3.1.6 Signature sequence for atypical substrates .....	23

3.1.7 Phylogenetic analysis.....	24
3.2. Water transport activity .....	25
3.3 Growth assays.....	29
3.3.1 Growth assays under osmotic stress and atypical substrates.....	29
3.3.2 Growth assays under osmotic stress and atypical substrates in liquid media .....	30
4. Discussion .....	34
5. Concluding remarks and Future perspectives .....	37
6. References .....	38
Annexes.....	45

## List of figures

Figure 1.1. - Cork oak (a), its acorns (b) and detail of the cork (c). (Modesto, 2012)

Figure 1.2 - Cork oak distribution (Berrahmouni, Regato, & Stein, 2007).

Figure 1.3 - Typical structure (monomer) of an aquaporin subunit (Kruse et al., 2006)

Figure 1.4 - Representation of the aquaporin structure. Each monomer is constituted by 6 transmembrane helices connected by 5 loops. Both B and E loops contain highly conserved NPA motifs whose interaction forms a pore, allowing water to pass (Badaut, Lasbennes, Magistretti, & Regli, 2002).

Figure 1.5 - Microscopic photography of *Saccharomyces cerevisiae* cells.

Figure 2.1 – Schematic representation of the cloning strategy used for obtaining the recombinant plasmids.

Figure 3.1 - PCR amplification with various cDNAs of *Q. suber* L. for amplification of TIP2;1 (**A**) and PIP2;4 (**B**). Picture A: 1 – negative control; 2 – G1; 3 – G2 ; 4 – A1; 5 – A2; 6 – ladder I; 7 – A5; 8 – HL2; 9 – HL3; 10 – HL4; 11 – HL5; 12 – positive control. Picture B: 1 – negative control; 2 – G1; 3 – G2 ; 4 – A1; 5 – ladder I; 6 – A2; 7 – A5; 8 – HL2; 9 – HL3; 10 – HL4; 11 – HL5. Arrows indicate the chosen cDNAs to proceed for further analysis.

Figure 3.2 - Insert analysis of *Q. suber* L. TIP 2;1 (A) and PIP 2;4 (B). **A** - Lane 1: Religation, Lane 2: A1, Lane 3: A2, Lane 4: A3, Lane 5: A4, Lane 6: A5, Lane 7: B1, Lane 8: Religation, Lane 9: B2, Lane 10: B3, Lane 11: B4, Lane 12: B5, Lane 13: C1, Lane 14 : C2, Lane 15: C3, Lane 16: Religation, Lane 17: Religation, Lane 18: C4, Lane 19: D1, Lane 20: D2, Lane 21: D3, Lane 22:E1, Lane 23: Religation, Lane 24: E2, Lane 25: E3, Lane 26: F1, Lane 27: F2, Lane 28: F3, Lane 29: Religation. **B** – Lane 1: Clone A1; Lane 2 – Clone A2; Lane 3 – A3; Lane 4: A4; Lane 5 – A5; Lane 6 – B1; Lane 7 – B2; Lane 8: Religation; Lane 9 – B3; Lane 10 – B4; Lane 11 - B5; Lane 12 – C1; Lane 13 – C2; Lane 14 – C3; Lane 15 – C4; Lane 16 – C5; Lane 17 – D1; Lane 18 – D2; Lane 19 – D3; Lane 20 – D4; Lane 21 – D5; Lane 22 – E1; Lane 23 – E2; Lane 24 – Religation; Lane 25 – E3; Lane 26 – E4; Lane 27 – E5; Lane 28 – F1; Lane 29 – F2; Lane 30 – F3; Lane 31 – F4; Lane 32 – F5. Arrows indicate the clones chosen for following clone analysis.

Figure 3.3 - Clone analysis of TIP2;1 clones by PCR (A) and by digestion (B) and Clone analysis of PIP 2;4 clones by PCR (C) and by digestion (D). **(A)** and **(B)**: Lane 1 – Ladder; Lane 2 – Clone A2; Lane 3 – Clone B2; Lane 4 – Clone C1; Lane 5 – Clone C4; Lane 6 – Clone E1; Lane 7 – Clone F1; Lane 8 – Positive Control And Lane 9 – Negative Control. **(C)**: Lane 1 – Positive Control; Lane 2 – Clone A1; Lane 3 – Clone A2; Lane 4 – Clone B2; Lane 5 – Clone B3; Lane 6 – Clone D3; Lane 7 – Clone E3 And Lane 8 – Ladder. **(D)**: Lane 1 – Positive Control; Lane 2 – Clone A1; Lane 3 – Clone A2; Lane 4 – Ladder; Lane 5 – Clone B2; Lane 6 – Clone B3; Lane 7 – Clone D3; Lane 8 – Clone E3.

Figure 3.4 - Localization of GFP-tagged aquaporins from *Q. suber* expressed in *S. cerevisiae* strains. Cytosolic GFP localization in **(A)** control **(B)** QsTIP2;1 **(C)** QsPIP2;4 A **(D)** QsPIP2;4 B. Images were taken under phase contrast (lower panel) and fluorescence (upper panel) microscopy.

Figure 3.5 - Sequencing results and database sequence aligned with Clustal X model on Bioedit.

Figure 3.6 - Weblogo image displaying the conserved Histidine in position 193. For this analysis 44 sequences were used. Accession numbers of the sequences used: POE96352, POE66465, POE97127, XP\_023923839, XP\_023923152, XP\_023870587, POF11915, XP\_023926845, XP\_023926844, XP\_023887849, XP\_023899033, CAO41326, CAO62835, CAO39626, CAO41326, CAN75442, CAO47394, CAO18152, CAO21844, KJ697714, KJ697715, KJ697716, P61837, Q06611, Q08733, Q39196, Q8LAA6, P43286, P43287, P30302, Q9FF53, Q9SV31, Q9ZV07, P93004, Q9ZVX8, AFH36339, AFH36340, AFH36341, AFH36336, AFH36337, AFH36338, ACV70047, ACV70053, ACV70055.

Figure 3.7 - Weblogo image displaying the conserved Serine in position 274. In this analysis 24 sequences were used. Accession numbers of the sequences used: POF11915, XP\_023926845, XP\_023926844, XP\_023887849, XP\_023899033, POE92575, XP\_023899033, CAN75442, CAO47394, CAO18152, CAO21844, KJ697715, KJ697716, P43286, P43287, P30302, Q9FF53, Q9SV31, Q9ZV07, P93004, Q9ZVX8, AFH36336, AFH36337, AFH36338.

Figure 3.8 - Weblogo image displaying the conserved Serine in position 274. In this analysis 30 sequences were used. Accession numbers of the sequences used: POE65492, XP\_023920799, XP\_023904770, POE73559, XP\_023903922, POF05546, POE96780,

CAO69259, CAO63006, CAO16745, CAO21720, CAO23095, CAO44039, CAO42713, CAO70596, KJ697717, HQ913640, P25818, Q41963, O82598, Q41951, Q41975, Q9FGL2, P26587, O22588, O82316, Q9STX9, AFH36342, AFH36343, AFH36344.

Figure 3.9 - Weblogo image displaying the conserved Threonine in position 97. In this analysis 21 sequences were used. Accession numbers of the sequences used: POE65492, XP\_023920799, POE73559, XP\_023903922, POE96780, CAO69259, CAO63006, CAO16745, CAO21720, CAO45860, CAO23095, CAO44039, KJ697717, HQ913640, P25818, Q41963, O82598, Q41951, Q41975, Q9FGL2, P26587, AFH36343, AFH36344.

Figure 3.10 - Weblogo image displaying the conserved Histidine in position 131. Accession numbers of the sequences used: XP\_023903922, POF05546, CAO45860, CAO23095, CAO44039, CAO42713, HQ913640, Q41951, Q41975, Q9FGL2, O82316, AFH36342, AFH36343.

Figure 3.11 - Signature sequences for atypical substrates, boron and hydrogen peroxide. Arrows identify the sequences obtained in this study.

Figure 3.12 - Phylogenetic tree obtained with Neighbor-Joining method, bootstrap and 1000 replicates. Arrows point to the sequences obtained in this study. Accession numbers of the used sequences: POE65492, XP\_023920799, XP\_023904770, POE73559, XP\_023903922, POF05546, XP\_023889965, XP\_023889944, POE96780, XP\_023917997, POE96352, XP\_023888245, POE66465, XP\_023923839, XP\_023923152, XP\_023870587, POE77117, POF11915, XP\_023919491, POF21789, POF21792, POF01595, XP\_023926844, XP\_023887849, POE92575, XP\_023899033, AFH36339, AFH36340, AFH36341, AFH36336, AFH36337, AFH36338, AFH36342, AFH36344, ACV70039, ACV70047, ACV70053, CAO41326, CAO62835, CAO39626, CAO41326, CAN75442, CAO47394, CAO18152, CAO21844, CAO69259, CAO63006, CAO16745, CAO21720, CAO45860, CAO23095, CAO62035, CAO44039, CAO42713, CAO70596, P61837, P61837, Q08733, Q39196, Q8LAA6, P43286, P43287, P30302, Q9FF53, Q9SV31, Q9ZV07, P93004, Q9ZVX8, P25818, Q41963, O82598, Q41951, Q41975, Q9FGL2, P26587, O22588, O82316, Q9STX9.

Figure 3.13 - Water permeability coefficients ( $P_f$  at 23°C) of QsTIP2;1 and QsPIP2;4 A were higher. Expression of QsPIP2;4 B did not increase water permeability in yeast cells. Data are mean  $\pm$  SD of three independent experiments.

Figure 3.14 - Arrhenius plot of  $P_f$  at temperature range (11–34°C), where T is temperature in Kelvin.  $E_a$  was evaluated from the slopes. Empty plasmid (pUG35) showed steeper slope, while strains expressing QsTIP2;1 and Qs PIP2;4 A exhibited shallow slope.

Figure 3.15- Water permeability coefficients ( $P_f$  at 23°C) of QsTIP2;1 was reduced by 0.5mM of Mercury chloride, while QsPIP2;4 A increased. Data are mean  $\pm$  SD of two independent experiments.

Figure 3.16 - Water permeability of QsPIP2;4A in the presence of mercury and BME

Figure 3.17 - Phosphorylation effect on QsTIP2;1 QsPIP2;4 A and QsPIP2;4 B.  $P_f$  value at pH 5.0 slightly reduced the water permeability of all *Quercus suber* L. and empty plasmid.

Figure 3.18 - Water permeability of yeast strains expressing QsTIP2;1, QsPIP2;4 A and QsPIP2;4 B. permeability coefficient ( $P_f$ ) was measured at intracellular pH 6.8, pH 5 and pH 5 + benzoic acid.

Figure 3.19 - Growth assays of *S. cerevisiae* strains expressing *Q. suber* aquaporins under osmotic stress and atypical substrates. Yeast strain transformed with empty pUG35 plasmid was used as control (pUG35). Yeast suspensions were spotted in 10-fold dilution on solid YNB plates with 2.1 M sorbitol. Growth was recorded after two weeks at 28°C.

Figure 3.20 - Growth curve of all yeast strains on YNB+2% glucose+LTH (control conditions).

Figure 3.21 - Growth curve of all yeast strains on YNB+2% glucose+LTH and 2.1M sorbitol. This conditions were meant to evaluate the effect of the osmotic stress.

Figure 3.22 - Growth curve of all yeast strains on YNB+2% glucose+LTH and 40mM Boric acid. This conditions were applied to observe the transport of boron.

Figure 3.23 - Growth curve of all yeast strains on YNB+2% glucose+LTH and 0.25mM H<sub>2</sub>O<sub>2</sub>. This conditions were applied to observe the transport of hydrogen peroxide.

Figure 0.1 - Gradient PCR with A2 cDNA. From lane 1 to lane 10 temperature rises from 50°C to 60°C and then from 55°C to 65° in the second cycle. Lane 6 is ladder and lane 11 is positive control

Figure 0.2 - Result of gel-purification of TIP2;1 aquaporin (A) and PIP2;4 (B).

Figure 0.3 - Result of purification after digestion of TIP2;1 (A) and PIP2;4 (B)

Figure 0.4 - Plasmid extraction of transformants cloned with TIP 2;1 (A) and PIP2;4 (B). (A): lane 1 – A2; lane 2 – B2; lane 3 – ladder and lane 4 – F1. (B): lane 1 – lambda hind III; lane 2 – A1; lane 3 – A2; lane 4 – B2; lane 5 – B3; lane 6 – D3 and lane 7 – E.  
Figure 0.5 - pUG35 plasmid map.

## List of tables

Table 2.1 - List of samples with their origin's localization

Table 2.2 - Primers used in this study.

Table 2.3 - PCR program used to amplify the gene sequences.

Table 3.1 - Growth parameters of QsTIP2;1, QsPIP2;4 A and QsPIP2;4 B obtained for growth in liquid media under osmotic stress and atypical substrates

## List of Abbreviations

ABA – Abscisic Acid  
AQP – aquaporin  
AQY – yeast aquaporin  
Arg – arginine  
At – *Arabidopsis thaliana*  
ATP – Adenosine Triphosphate  
BME –  $\beta$  – mercaptoethanol  
CFDA – 5 – (and 6) – carboxyfluorescein diacetate  
Cys – Cysteine  
Ea – Activation energy  
GFP – Green Fluorescent Protein  
Hist – histidine  
Leu – Leucine  
Lys – lysine  
MIP – Major Intrinsic Protein  
NADH - Nicotinamide Adenine Dinucleotide  
OD – Optic Density  
Os – *Oryza sativa*  
PCR – Polymerase Chain Reaction  
pH<sub>in</sub> – intracellular/intracellular pH  
pH<sub>out</sub> – Extracellular pH  
PIP – Plasma membrane Intrinsic Protein  
Qs – *Quercus suber*  
Ser – Serine  
Thr – Treonine  
TIP – Tonoplast Intrinsic Protein  
TMH – Transmembrane Helix  
VvPn – *Vitis vinifera* Pinot noir  
VvTn – *Vitis vinifera* Touriga nacional  
YNB – Yeast Nitrogen Base  
YPD – Yeast extract Peptone Dextrose

# 1. Introduction

## 1.1 *Quercus suber* L.

Cork oak (*Quercus suber* L.) is a Mediterranean tree, extremely long living and slow growth belonging to the *fagaceae* family. This tree has separate male and female flowers, pollinated by wind and propagated mainly by natural regeneration and acorn producing, which means it depends on gravity and animals to spread (Modesto, 2012). The remarkable detail about this tree is the cork, a thick and porous accumulation of cells filled with cellulose, lignin, suberin, tannin and waxes (Gil, 2015). This special bark is continuously being produced and confers protection against abiotic factors (Modesto, 2012).



Figure 1.1. - Cork oak (a), its acorns (b) and detail of the cork (c). (Modesto, 2012)

The cork oak is only found in the western Mediterranean countries, like Portugal, Spain, Tunisia, Italy, Algeria and France. This species is an important resource with ecological (water cycle, soil protection, carbon sequestration and as reservoir of biodiversity) and socioeconomic impact, especially in Portugal, which has the biggest cork oak forest and is the main cork producer (Pereira-Leal et al., 2014). Cork oaks have high ecological importance because they form an ecological system named “montado” (in Portugal) or “dehesa” (in Spain), which is managed by man. These woodlands have low tree density and are used for the production of cork but also for cattle grazing and hunting. The restricted location of the cork oaks is mainly related to their soil preferences for acidic and non-calcareous soils (Modesto, 2012).

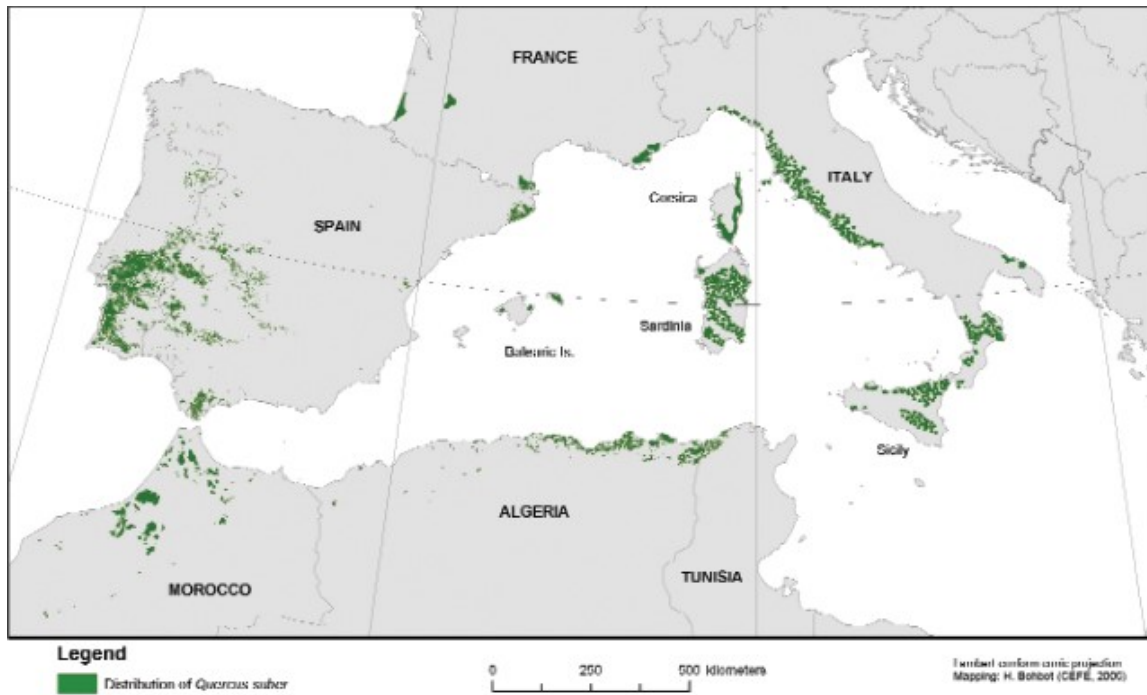


Figure 1.2 - Cork oak distribution (Berrahmouni, Regato, & Stein, 2007).

Oaks have been considered as relevant to study the adaptation mechanisms as they thrive under extreme conditions. However, cork oak population has declined over the years and it has been predicted that the diseases affecting them might expand to other areas (Pereira-Leal et al., 2014).

## 1.2 Aquaporins

Water homeostasis is a fundamental aspect for the survival and adaptation of all living beings, and their efficient transport through the cellular membrane is prerequisite under all the cellular condition for survival and adaptation.

For a long time, it was believed that water passed only through the membrane lipids, in a process with high activation energy (Li, Santoni, & Maurel, 2014). However, after the discovery of a class of water-transport proteins named aquaporins in erythrocytes, the concept of membrane water permeability became more clear (Maurel, Végétales, & Terrasse, 1997). Nowadays, it is known that there are two ways for water to pass through the biological membranes: through the membrane lipids by passive diffusion, and through specific transporters, the aquaporins, in a process with low activation energy and of particular relevance to the cells when they are subjected to low temperatures (Maurel, Verdoucq, & Luu, 2008).

Even though the main function of most described aquaporins is the water transport, they also play a role in the transport of small molecules, such as gases (CO<sub>2</sub>, NH<sub>3</sub>) (Maurel et al., 2008; Uehlein, Lovisoló, Siefritz, & Kaldenhoff, 2003), small solutes (H<sub>2</sub>O<sub>2</sub>) (Sabir et al., 2014), boron (Mosa, Kumar, Chhikara, Musante, & White, 2016) and ions (K<sup>+</sup> e Cl<sup>-</sup>) (Sabir et al., 2014).

### 1.2.1 Structure of aquaporins

Aquaporins are pore forming small integral membrane proteins that belong to the ancient family of major intrinsic proteins (MIPs) in animals, microorganisms, and plants (Maurel et al., 2008). These proteins are composed by four identical subunits in which every subunit presents six transmembrane domain in alpha helices (TM1 – TM6) connected by 5 *loops* (A to E) placed intra or extracellularly (Kruse, Uehlein, & Kaldenhoff, 2006), having the N-terminal and C-terminal regions both located in the cytosol (Maurel et al., 2008). Three of the connecting loops are placed extracellularly (*loops* A, C and E) and the other two in the cytosol (*loops* B and D) (Soveral, Trincão, & Moura, 2011) (Figure 1.3). The protein comprises two internal tandem repeats, covering roughly the amino- and carboxy-terminal halves of the protein. Each repeat consists of three transmembrane helices and a highly conserved loop following the second transmembrane helix (*loops* B and E, respectively). These loops include a conserved signature motif, asparagine-proline-alanine (NPA). *Loops* B and E form short helices that fold back into the membrane, with *loop* B entering the membrane from the cytoplasmic side and *loop* E from the extracellular side. A seventh transmembrane domain in which the two NPA boxes are orientated 180 degrees to each other is thus formed, creating an aqueous pathway through the proteinaceous pore (Kruse et al., 2006) (Figure 1.4).

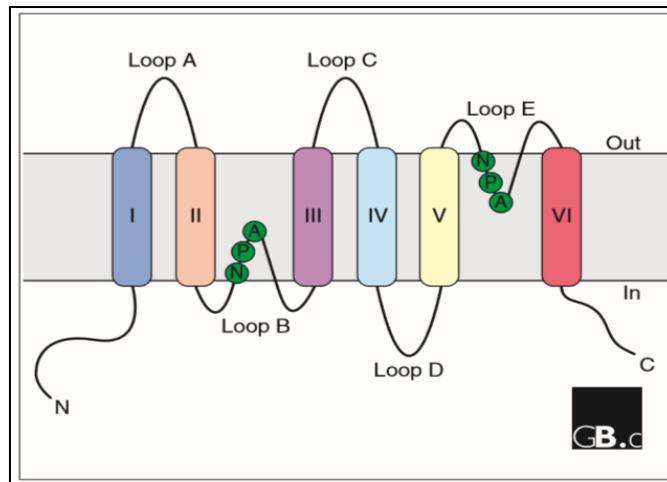


Figure 1.3 - Typical structure (monomer) of an aquaporin subunit (Kruse et al., 2006)

The pore is formed by the helices and *loops* B and E that contain a highly conserved NPA motif (Filter 1) (Figure 1.4), where the presence of particular residues confers size constrictions and charge characteristics that allow water to flow. Besides, a specific recognition of the substrate mediated by space boundaries is defined by hydrogen bonds and by hydrophobic interactions within the pore (Filter 2, aromatic constriction/Arginine) (Forrest & Bhawe, 2007; Wallace & Roberts, 2004). Furthermore, close to the second NPA, a serine (Ser) is also involved which has also been identified as being part of the selectivity (Froger, Tallur, & Thomas, 1998; Heymann & Engel, 2000). The impermeability of aquaporins to protons can be explained by electrostatic repulsion, orientation of the dipole and isolation of the water molecule when it passes through the center of the pore (Forrest & Bhawe, 2007).

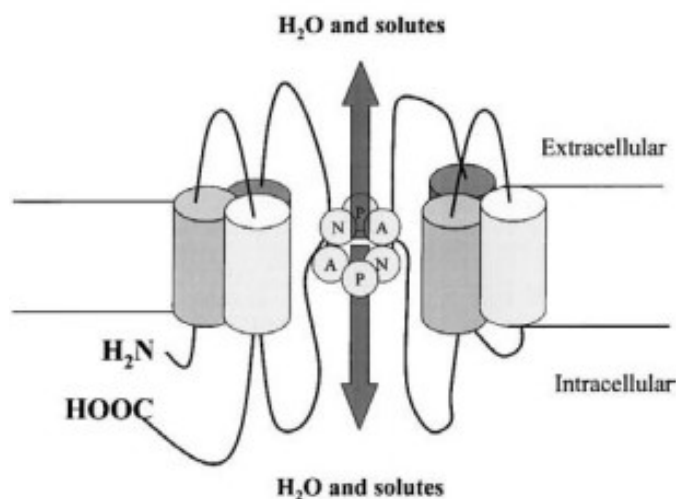


Figure 1.4 - Representation of the aquaporin structure. Each monomer is constituted by 6 transmembrane helices connected by 5 loops. Both B and E loops contain highly conserved NPA motifs whose interaction forms a pore, allowing water to pass (Badaut, Lasbennes, Magistretti, & Regli, 2002).

### 1.2.2 Water transport in plants

Plants, like any other living being, are constituted mainly by water (75-85%)(Taiz & Zeiger, 2002).

In plants, water promotes the absorption of the dissolved minerals in the soil, it helps moving the solutes for and from the cells, participates in biochemical reactions (like photosynthesis) and it has influence over the molecular structures of proteins (Calamita, 2005). Despite being sessile, plants have to absorb water and minerals from their close environment (Maurel et al., 2015), so they have developed mechanisms to capture and transport water and minerals from the root to adapt to their environment and to various stress factors (Taiz & Zeiger, 2002). Because they have no way of moving, plants have to endure several constraints from both aerial and soil environments. These conditions may be abiotic stresses, like lack or excess of water, or mineral ions in the soil, that can be either beneficial or toxic. Extremes in temperature, either high or low, can also be stressful for the plants, especially in the shoot. However, plants not only face abiotic stress but also biotic. They can be attacked by herbivores, insects and pathogenic microorganisms (Maurel et al., 2015).

The gradient of water potential ( $\Delta\Psi$ ) drives the water movement, and water goes from where  $\Psi$  is higher to where it is lower (F. Chaumont & Tyerman, 2014). The most relevant mechanism for the water flow maintenance in plants is the transpiration, during which an intense flow of water travels through the plant body, from the root through the opened stomata, where it evaporates (Maurel et al., 2015). This flow decreases the leaf  $\Psi$  and causes water to move from the xylem toward the leaf surface (F. Chaumont & Tyerman, 2014). This type of water movement is very important and useful to deliver water and nutrients to the upper part of the shoot. However, water uptake in roots and its deliver to shoots requires transport by living cells (Maurel et al., 2015).

### 1.2.3 Aquaporins from plants

Since the aquaporins were first discovered in *Arabidopsis thaliana* and their characterization as water channels in *Xenopus* oocytes, many other aquaporin coding genes were identified in other plant species (mayze and rice, for example) (Maurel et al., 2015). The water permeability increase of the membrane after heterologous expression of these proteins in oocytes, has shown that aquaporins represent an important selective pathway for the water movement trough the membrane. In plants, the water transport by aquaporins has been considered as fundamental in important physiological processes, like elongation, germination of seeds and osmoregulation (Maurel, 2007).

In plants, the genes encoding aquaporins are very abundant. These show greater diversity than their homologues in the animals, both in relation to the substrates and the expression profiles, regulation and intracellular localization (Forrest & Bhave, 2007; Maurel et al., 2008), which was attributed to the higher level of compartmentalization of plant cells and their greater need to control water contents (Kruse et al., 2006). Aquaporins also allow a rapid and reversible water

transport, so they can exert a vital function when the plant is facing water stress (François Chaumont, Moshelion, & Daniels, 2005).

Plant aquaporins are subdivided into seven subfamilies; PIPs (Plasma membrane Intrinsic Protein), TIPs (Tonoplast Intrinsic Protein), NIPs (Nodulin-26-like Intrinsic membrane Protein), which can also transport glycerol and are considered an aquaglyceroporin, SIPs (Small basic Intrinsic Protein), GIPs (GlpF-like), HIPs (Hybrid Intrinsic Proteins) and XIPs (X Intrinsic unclassified Proteins) although some are only present in specific plant groups (Laloux et al., 2018).

#### PIP subfamily

As the name says, PIP aquaporins are highly expressed in the plasma membrane. Members of this family have a molecular weight of around 30 kDa and within the PIP-type aquaporins present in plants, two subgroups, PIP1 and PIP2, can be pointed. PIP 1 group has 5 isoforms (PIP1;1 to PIP1;5) and PIP2 has 8 isoforms (PIP2;1 to PIP2;8) (Maurel, 2007). Although presenting a similar basic structure, PIP1 and PIP2 exhibit a notorious difference: PIP1 aquaporins have a longer N-terminal but shorter C-terminal when compared to PIP2. However, all PIPs have a conserved serine believed to be essential for the opening and closing of the phosphorylation-regulated channel (Kjellbom, Larsson, Johansson, Karlsson, & Johanson, 1999; Schaffner, 1998).

Despite their sequence identity, transport activity varies between these two groups. PIP1 are considered as non-functional in most plant species, while PIP2 group are known to be efficient water transporters. However, when PIP1 and PIP2 are co-expressed, an increase of the water permeability is observed. This happens because PIP1 and PIP2 members interact with each other resulting in hetero-tetramerization of both isoforms (Vajpai, Mukherjee, & Sankararamakrishnan, 2018). Increase of permeation in co-expression has been observed in many plants, including maize (Vajpai et al., 2018) and grapevine (F. Sabir, personal information).

#### TIP subfamily

The TIP-type aquaporins are mostly expressed on the membrane of the tonoplast and have a molecular weight of 25 to 28 kDa. In rice, maize and Arabidopsis, TIPs can be subdivided into five subgroups: TIP1, TIP2, TIP3, TIP4 and TIP5 (Gerbeau, Güçlü, Ripoche, & Maurel, 1999). Some of its isoforms are related only to certain organs or stages of development, for example the expression of AtTIP2;1 is very high in the aerial part but almost non-existent in the root (Daniels, 1996). Members of TIP4 group can transport solutes other than water, as demonstrated for NtTIP4 (Gerbeau et al., 1999) and for VvTnTIP4;1 (Sabir et al., 2014).

Since the vacuole occupies 90% of the cell volume, TIPs are indicated as essential for the intracellular movement of water, the regulation of turgor pressure (Shapiguzov, 2004) and cell growth processes (F. Chaumont & Tyerman, 2014).

#### 1.2.4 Physiological role of aquaporins in the transport of unconventional solutes and resistance to abiotic stresses

Initially, aquaporins were thought to be channels specific for water transport, but more recently, assays performed with various aquaporins expressed heterologously in yeasts and *Xenopus* oocytes (Ishikawa, Suga, Uemura, Sato, & Maeshima, 2005; Maurel, Reizer, Schroeder, & Chrispeels, 1993) have shown that plant, animal and yeast aquaporins can also transport small neutral solutes, for example glycerol (Biela et al., 1999), boron (Fujiwara, Takano, Wada, Ludewig, & Schaaf, 2006), H<sub>2</sub>O<sub>2</sub> (Bienert et al., 2007) and others (Gerbeau et al., 1999). These observations led to a classification of aquaporins as orthodox aquaporins and heterodox aquaporins (Soveral, Prista, Moura, & Loureiro-Dias, 2011). The orthodox aquaporins transport exclusively water, while heterodox aquaporins transport other small solutes besides water (Takata, Matsuzaki, & Tajika, 2004).

Boron is an essential nutrient for plant growth. It is taken up from the soil and its main functions are related with cell wall reinforcement, nucleic acid synthesis, hormone responses, membrane functions and cell cycle regulations (Maurel et al., 2015; Mosa et al., 2016). While essential, excess boron in the soil or water can be toxic for the plants, as it can lead to nutritional unbalances that eventually limits the plant growth (Mosa et al., 2016). Studies have shown that AtNIP5;1 is essential for boron uptake in limiting conditions (Maurel et al., 2015).

Besides from being a potential threat to living cells, H<sub>2</sub>O<sub>2</sub> also acts as an activator of the Ca<sup>2+</sup> channels required for root hair growth and stomata regulation. Under stress, H<sub>2</sub>O<sub>2</sub> can be compartmentalized inside the cells and in the apoplastic regions. In fact, TIPs are suggested to transport H<sub>2</sub>O<sub>2</sub> to the vacuoles for further detoxification by peroxidases (Kalam, Yoshikawa, Ishikawa, Sawa, & Shibata, 2012).

In addition to water transport at the plant level, aquaporins are also involved in regulating turgor pressure and intracellular water movements. During water stress, the low efflux of water leads to low turgor pressure of the cell. In this situation, the cytosol is very sensitive to water exchange through the plasma membrane and tonoplast, but abrupt changes in cytosolic volume can be avoided if there are changes with the vacuole (Javot & Maurel, 2002). Therefore, it was proved that, in case of water stress, the activity of the aquaporins in the tonoplast is much higher than normal condition (Maurel et al., 1997). Osmotic stress also requires an adaptation of the membrane. Studies have shown that, initially cell permeability was very low but was dynamically adjusted during mobilization of material at the cell surface (Moshelion, Moran, & Chaumont, 2004).

#### 1.2.5 Regulation

The regulation of the biological membrane to water permeability is a very complex process. There can be mechanisms of rapid control which directly affect the aquaporin activity or slower adaptive responses at gene expression level. Several control mechanisms, such as salt stress, osmotic stress and water availability can determine the opening and closing of the channel,

representing a rapid control mechanism (François Chaumont et al., 2005). Aquaporin activity can be modified by heavy metals, and mercury, specially, has been proved to inhibit aquaporin activity (Maurel et al., 2015; Sabir et al., 2014). Mercury inhibition is taught to occur by its binding to the thiol groups of particular Cys residues. However, this inhibition has been questioned, since some aquaporins are insensitive (because they do not have the specific Cys residues) and SoPIP2;1 has its activity enhanced by mercury (Frick et al., 2013). One possible explanation is related to the binding of mercury to three out of four cysteine residues, Cys<sup>91</sup> in the end of helix 2, Cys<sup>127</sup> and Cys<sup>132</sup> in helix 3 but no differences were observed when mutants were created by changing the cysteines into serines, either by changing every cysteine singularly or by constructing double and triple mutants, so it is possible to assume that these residues are not the reason why mercury activates this aquaporin (Frick et al., 2013).

Another group of researchers, Kirscht and her group, tried to explain mercury effect using a different approach. Since Cys was thought to have a structural function in this aquaporin and not to be a binding site for mercury, they tried to prove this hypothesis and found that, when this cysteine was replaced by a serine or an alanine, the permeability of the aquaporin increased and, proportionally, it also increased after mercury application (Kirscht, Survery, Kjellbom, & Johanson, 2016). This fact was explained by the destabilization of the dimer, since serine is able to form hydrogen bonds but alanine isn't, and this would compensate the disulfide bond. This destabilization of the dimer might result in a relaxation of the selectivity filter and therefore increasing the permeability (Kirscht et al., 2016). The same group has also hypothesized that mercury can cause tryptophan to quench and this is usually related to rearrangements of the proteins. They observed that tryptophan 35 and 38 have different positions in open and closed conformation stating that in open conformation tryptophan 35 might release C-terminus (Kirscht et al., 2016). It has also been suggested that the mercury might cause the decrease of the lipid bilayer fluidity and that this mechanical stimuli might regulate the SoPIP2;1 (Frick et al., 2013). Besides, OsNIP3;3 has also showed increased activity when mercury chloride was added and also in this case, the cysteines appeared not to have influence in this. However, the group suggests that it might be related to the His<sup>168</sup> in *loop C*, where mercury can bind and modify the path for water transport (Katsuhara et al., 2014). Despite the numerous hypothesis, a more recent work suggests that the activation by mercury chloride might be by direct binding to the aquaporin (Kirscht et al., 2016).

The gating mechanism for PIP group has been proposed, based on SoPIP2;1, by Törnroth-Horsefield and her co-workers in 2006 (Törnroth-Horsefield et al., 2006). The model they proposed indicates a reversible motion of a Leu residue can open and close the pore. In the open conformation, *loop B* is distal from *loop D*. However, when the His residue (in *loop D*) is protonated, it allows an interaction between this residue and the Asp residue of the N-terminal region. This causes a displacement of *loop D*, driving to a conformational change which covers the pore with the Leu residue (Maurel et al., 2015).

In the PIPs, phosphorylation conserved in *loop B* and adjacent to the C-terminal tail have been observed (Maurel et al., 2008). In fact, the phosphorylation of a Ser residue in *loop B* disrupts

the interactions between *loop B* and *loop D*, making the aquaporin have an open conformation (Maurel et al., 2015). Phosphorylation in the Ser residue of the C-terminal region breaks the hydrogen bond of it with some neighbor protomer residues and stabilizes *loop D* (Frick et al., 2013).

In PIP, the pore opening can be regulated through the cytosol, by protons or bivalent cations. The pH gating relies on the protonation of the His residue of *loop D*, as mentioned before. When pH is acid, the protonated His interact with other residues of *loop B* and stabilize the aquaporin in a closed conformation. Although this mechanism has been proved for PIPs, in TIPs there is also some reports of inhibition by pH and it involves a His residue in *loop C*. The mechanism, however, is still unknown (Maurel et al., 2015).

The inhibition of PIPs by divalent cations is related to a binding site in *loop B*, which mediates a bonding with the N-terminal and *loop D*, stabilizing the closed pore conformation. This mechanism has been observed with Cd<sup>2+</sup>, however, it is taught that in vivo, the binding site may be occupied by Ca<sup>2+</sup> (Maurel et al., 2015).

In TIPs, it has been proved that membrane tension regulates their permeability. There is increasing evidence that the pressure in the membrane inhibits the permeability of the aquaporins to water, such as for AQP-1, VvTnTIP2;1 and AQY-1 (Leitão, Prista, Loureiro-Dias, Moura, & Soveral, 2014; Ozu, Dorr, Gutiérrez, Teresa Politi, & Toriano, 2013; Soveral, Madeira, Loureiro-Dias, & Moura, 2008). Since the vacuole's increase of volume is related to the transport of osmotically active components associated with a rapid influx of water, which creates the internal turgor pressure, pressure depending membrane tension can be a mechanism of regulation of the vacuolar size and shape (Leitão et al., 2014).

Besides from phosphorylation, methylation, deamidation, NH<sub>2</sub>-terminal acetylation and ubiquitination have been found and point to a variety of regulation mechanisms targeting aquaporin expression and function. However, besides from phosphorylation, the significance of the post-translational modifications is not clear (Maurel et al., 2015).

Studies have shown that the gene transcription of aquaporins can be modified by hormonal stimuli (ABA and gibberellin), low temperatures, water deficit, mineral deficit and, more interestingly, by light (Javot & Maurel, 2002). In fact, a change in the water permeability of *Samanea saman*'s (rain tree) protoplasts during the day was observed and correlated with PIP2 expression (Plant et al., 2002).

### 1.3 *Saccharomyces cerevisiae*

*Saccharomyces cerevisiae* is a species of yeast that has been very important in brewing, winemaking and baking since the dawn of times. There's proof that this yeast was used for beer brewing in Sumeria and Babylonia around 600 BC, which makes it, probably, the oldest domesticated organism. Although it was used by Egyptians and in Georgia in ancient times, it was only discovered in 1837 by Meyen in malt (Feldmann, 2010).

Yeast cells exhibit a great morphological heterogeneity and even the physical or chemical conditions of the growth media can lead to profound changes in the cell morphology. However,

under the microscope, *S. cerevisiae* cells appear as ovoid or ellipsoidal structures with a thick cell wall (Feldmann, 2010).

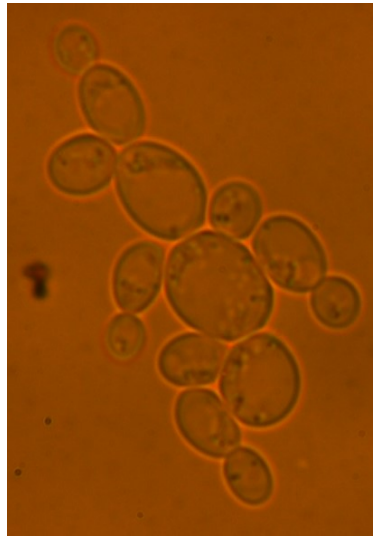


Figure 1.5 - Microscopic photography of *Saccharomyces cerevisiae* cells.

The major source of energy of this particular yeast is glucose and the pathway for conversion of glucose to pyruvate is glycolysis, where the production of energy in the form of ATP is bound to the generation of intermediate compounds and reducing power of NADH. The two major modes of use of pyruvate for energy production are respiration (in the presence of oxygen) and fermentation (absence of oxygen) (Feldmann, 2010).

Commonly known as budding yeast, *Saccharomyces cerevisiae*, is considered as one of the best currently known model organisms. It is classified as a unicellular fungus thus containing membrane-bound organelles, like nucleus and mitochondria (Duina, Miller, & Keeney, 2014). Unlike other, more complex, yeast, *S. cerevisiae* can be grown on defined media, which gives the investigator full control over the growth parameters (Feldmann, 2010). Yeast cells are able to divide as fast as once every 90 minutes. Due to that, to its microscopic size and to the fact that it is simple to grow, they are inexpensive and easy to work with in the laboratory. Yeasts form colonies on plates in just few days and don't require any special incubators or conditions. Its most distinguishing characteristic is the easiness researchers have to genetically change it (Duina et al., 2014).

The ease of manipulation of both the yeast and its genetic material has allowed to study in great detail many yeast functions. There are a great number of genetic manipulation protocols available, like transformation by lithium acetate method and electroporation. Also, many vectors for recombinant yeast have been designed and made available as well as yeast strains carrying auxotrophic markers, drug resistance markers, or defined mutations (Feldmann, 2010).

The success of this yeast as a model organism is also due to the fact that many processes have been conserved from yeast to mammals so it became a reference to which sequences of human, animal, or plant genes could be compared (Feldmann, 2010).

*Saccharomyces cerevisiae*, is very well-known heterologous expression system which has been proven useful for functional analysis of aquaporins (Leitão, Prista, Moura, Loureiro-Dias, & Soveral, 2012; Sabir et al., 2014) because of the low intrinsic water permeability of the plasma membrane. This system allows to overcome the main problems of tissue analysis, which are caused by the high cellular volume, low expression and activity levels and aquaporin activity under gene over-expression or deletion. In this yeast, growth assays can be performed quite easily and reveal how the aquaporins can enhance the absorption of some compounds (Maurel et al., 2015).

#### 1.4 Aims

*Quercus suber* L. is facing many challenges, especially related to climate changes, such as drought, extreme temperature and pests, but also continuously increasing population is putting pressure through overgrazing, over-harvesting and forest clearance, by changing to plantations that grow faster, by poor management, by land abandonment, and by urban development in coastal areas (Berrahmouni et al., 2007). Studies have shown that in the last years there has been a reduction in the adaptation capacity of cork oaks and an increase in the susceptibility of the ecosystems to climate changes (Surovy & Ribeiro, 2008). The Mediterranean region has been identified as one of the most prone to have its climate severely changed and with major risk to the environment and ecosystems, due to warmer and drier conditions (Giorgi & Lionello, 2008). These trends combined with incorrect soil management policies, are endangering the forest areas making them more sensitive to abiotic stresses (Berrahmouni et al., 2007). The decline of cork oaks has also been related to water stress, as trees show lower efficiency on using water which leads to a more evident oxidative damage since trees aren't able to effectively protect themselves (Alves, 2014; Besson et al., 2014).

The amount of water uptake is related to the root water uptake, leaf transpiration and cellular growth, which are in turn related to the capacity of the cell wall to extend. Thus, genes related to water stress, such as the water channels, have crucial role in growth regulation, survival and death processes of the tree in particular under stress conditions (Javot & Maurel, 2002).

In view of the above mentioned, this work aimed to understand *Quercus suber* L. aquaporin roles and regulation particularly in response to abiotic stresses.

More specifically, two genes of aquaporins (one PIP and one TIP) were cloned using a *S. cerevisiae* strain with non-functional aquaporins (*aqy-null* strain, low intrinsic water membrane permeability) in order to:

1. Clone and characterize two *Quercus suber* L. aquaporins (1 PIP and 1 TIP) by its individual heterologous expression in *aqy-null S. cerevisiae* strain;
2. Functional characterize the two *Quercus suber* L. aquaporins for water as well as for non-aqua substrates;
3. Identify of the regulatory mechanisms of water transport through selected *Quercus suber* aquaporins by mercury chloride, phosphorylation and cytosolic and external pH.

## 2. Materials and Methods

### 2.1 Biological Material

To amplify aquaporins, specific cDNA samples of *Quercus suber* (Table 2.1) were kindly provided by Professor Leonor Morais and Vera Inácio (ISA-ULisboa). cDNAs were used to avoid the presence of introns in our sequences.

DH5 $\alpha$  *E. coli* strain was used as competent cells for bacterial transformation.

The *S. cerevisiae aqy-null* strain YSH1172 (Genotype: 10560-6B aqy1::KanMX4 aqy2::HIS3) was used for the transformation.

Table 2.1 - List of samples with their origin's localization

Name of the sample	Origin
A1	Stem of 1 year old tree
A2	Stem of 2 years old tree
A5	Stem of 5 years old tree
HL2	Cork of 2 year old tree
HL3	Cork of 3 year old tree
HL4	Cork of 4 year old tree
HL5	Cork of 5 year old tree
G1	Periderm of young stem
G2	Periderm of young stem

### 2.2 Cloning and heterologous expression of *Q. suber* aquaporins in *Saccharomyces cerevisiae*

For *TIP2;1* and *PIP2;4*, based on 3' and 5' coding region, restriction sites for *Xba*I and *Sal*I were also incorporated in the forward and reverse primers, respectively. The designed primers were used to amplify the complete coding region of the desired aquaporins (Table 2.2). PCR amplification was carried out in an Eppendorff thermocycler with Thermo Scientific's 2XPhusion MasterMix according to the PCR program described in Table 2.3. The amplified PCR products were purified with Wizard SV Gel and PCR Clean-up kit (Sigma) according to the manufacturer's instructions and digested with enzymes *Xba*I and *Sal*I.

The centromeric plasmid pUG35 digested also with same enzymes was used for cloning, conferring C-terminal GFP tagging, MET25 promoter and CYC1-T terminator (Figure 2.1). This plasmid has an antibiotic resistance cassette, which confers resistance to ampicillin. After digestion, the DNA was purified and then ligated at different vector: insert ratios (1:1, 1:3 and 1:5) at 15°C overnight. PCR products were cloned into the corresponding restriction sites of pUG35 (behind MET25 promoter and in frame with GFP sequence and CYC1-T terminator), according to (Leitão et al., 2012).

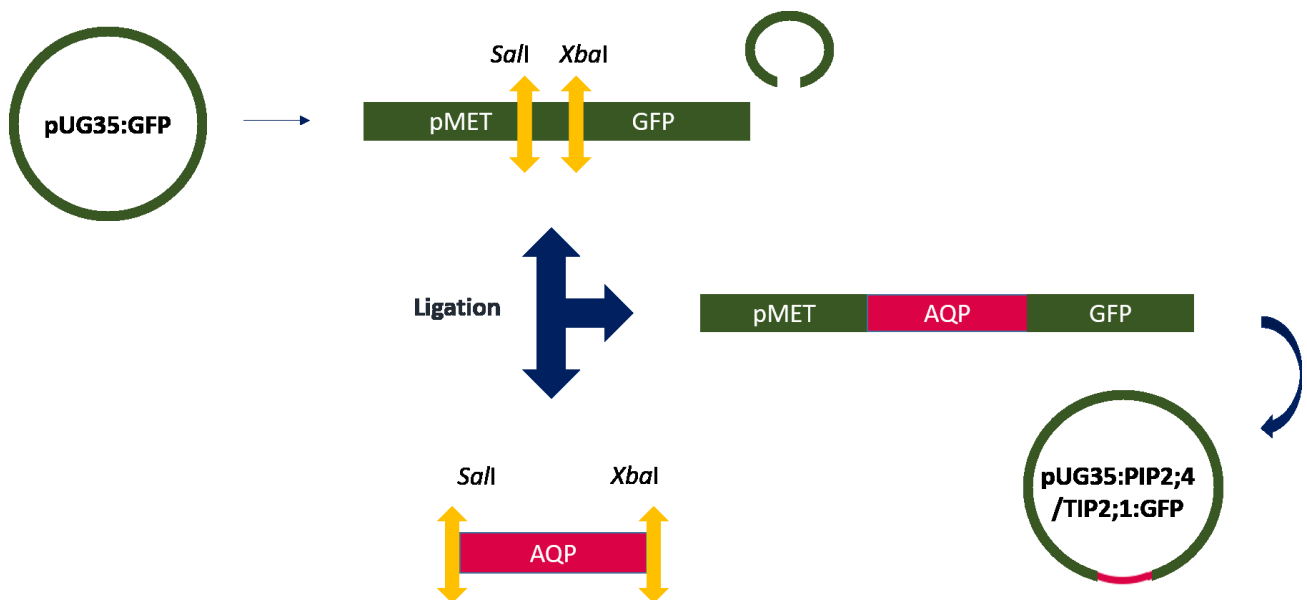


Figure 2.1 – Schematic representation of the cloning strategy used for obtaining the recombinant plasmids.

The recombinant plasmids were used to transform in *E. coli* (5  $\mu$ l and 10  $\mu$ l of each ligation ratio) and selected on LB plates supplemented with ampicillin. After one day of incubation at 37°C, colonies were then selected and inoculated in another LB with ampicillin media plate.

To confirm the presence of the amplicon in the plasmid of selected colonies, insert analysis was performed. DNA from the colonies was extracted with Phenol:Chloroform:Isoamyl alcohol (25:24:1) and ran on 1% agarose gel. Further on, in order to confirm if the insert is indeed the desired aquaporin gene in the plasmid, clone analysis was performed. For that, chosen clones were inoculated in liquid LB+ampicillin media to grow overnight. Thereafter, plasmid was extracted from the clones by alkaline-lysis method and desired insert was confirmed both by restriction digestion with *XbaI* and *SalI* and by PCR with primers designed from the flanking regions of the multicloning site of pUG35.

Selected plasmids were used for the transformation by the lithium acetate method according to Gietz and Schiestl (2007)(Gietz & Schiestl, 2007). *S. cerevisiae* cells were transformed with the plasmid of clones A2 and B2 for *PIP 2;4* and clone F1 of *TIP 2;1*. Yeast transformants were plated on YNB with 2% glucose and the supplements required for the auxotrophies and incubated at 30°C for 3 to 4 days. After four days, colonies were picked. Chosen clones were grown in liquid media in order to confirm the membrane localization of GFP-tagged aquaporins in *S. cerevisiae*, cells were taken at mid-exponential phase and were observed with Leitz Wetzlar Germany 513558 epifluorescence microscope equipped with a Leitz Wetzlar Germany Type 307-148002 514687 mercury bulb and BP 340–380; BP 450–490 (for GFP visualizing); BP 515–560 filter sets. Images were obtained with a digital camera Axiocam Zeiss using AxioVision Rel. 4.8.2 Software.

## 2.4 Sequence analysis

Plasmids of selected transformants were sent for sequencing to the company STABVIDA. DNA and protein sequences for comparative analysis were obtained from NCBI and Cork Oak DB (<http://corkoakdb.org>). Multiple protein sequence alignments were generated using BioEdit (Hall, 1999) programs and phylogenetic trees were obtained by using the MegaX (Kumar, Stecher, Li, Knyaz, & Tamura, 2018). Alignments were done using Clustal W (D.Thompson, G.Higgins, & J.Gibson, 1994) on BioEdit. The topology predicting was made using the EXPASY tools, such as TMHMM (Krogh, Larsson, Von Heijne, & Sonnhammer, 2001; Sonnhammer, Heijne, & Krogh, 1998) and TMPred (Ikeda, Arai, Okuno, & Shimizu, 2003).

The search of signature sequences for transport of atypical substrates was performed by aligning the obtained amino acid sequences with other sequences known to have those residues (Hove & Bhave, 2011). Images of conserved residues were generated by Weblogo (Crooks, Hon, Chandonia, & Brenner, 2004; D.Schneider & Stephens, 1990).

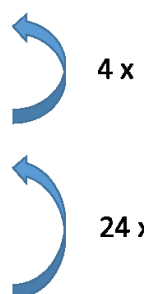
Gene	Primer Forward	T <sub>M</sub> (°C)	Primer Reverse	T <sub>M</sub> (°C)	Expected size (bp)
PIP2;4	<u>GGT</u> <u>AGCTCTAGA</u> ATGGCTGCCAAGGATATTG	61.5	ATAC <u>GC</u> <u>GCTGAC</u> ATGGCTGAAGAGCTC	64.1	804
TIP2;1	<u>GGT</u> <u>AGCTCTAGA</u> ATGGCCAGGATTGCCTTTGGTC	65.4	ATAC <u>GC</u> <u>GCTGAC</u> ATACTCATTGGACAGAGGTGCA TGTTTC	66.3	744
pUG35	CCTTCGTGTAATACAGGGTC	52.44	CACCTTTAGACATGTCGAGG	52.66	66+insert+25

Table 2.2 - Primers used in this study.

\* Restriction sites are underlined

Table 2.3 - PCR program used to amplify the gene sequences.

PCR PROGRAM	
94°C	2 minutes
94°C	30 seconds
60°C	1 minute
72°C	1 minute
94°C	30 seconds
65°C	1 minute
72°C	1 minute
72°C	7 minutes
4°C	hold



## 2.5 Water transport assays of *Q. suber* aquaporins expressed in *S. cerevisiae*

In order to functionally characterize cloned *Quercus* aquaporins, their water transport activity was estimated by stopped-flow spectroscopy (Soveral, Prista, et al., 2011). For that, cells are grown in YNB with 2% glucose and the amino acid supplements until mid-exponential phase (around OD<sub>640nm</sub> 1.0) and re-incubated for one hour in YPD medium. Then, cells were centrifuged and resuspended in 1.4M sorbitol and kept on ice for at least 90 minutes. After that, cells were loaded with the non-fluorescent dye 5-(and-6)-carboxyfluorescein diacetate (CFDA), which is hydrolyzed intracellularly and produces fluorescence. For the assays, hyperosmotic shocks were applied with HI-TECH Scientific PQ/SF-53 apparatus, in which equal amount of equilibrated cells and a 2.1M sorbitol solution were mixed, conferring the hyperosmotic shock, resulting in efflux of water and eventually causing cell shrinkage. This change in cell volume caused change in fluorescence intensity. The program associated allows to calculate the rate constant (k) which is then used to calculate the permeability coefficient ( $P_f$ ) based on the linear relationship between  $P_f$  and k as follows:  $P_f = k(V_0/A)[1/V_w(\text{osm}_{\text{out}})]$ , where  $V_w$  is the molar volume of water,  $V_0/A$  is the initial volume-to-area ratio and  $(\text{osm}_{\text{out}})$  is the final medium osmolarity (Soveral, Prista, et al., 2011).

Stopped-flow experiments were performed at temperatures ranging from 11 to 34°C. The activation energy ( $E_a$ ) of water transport was evaluated from the slope of Arrhenius plots ( $\ln P_f$  as a function of  $1/T$ ).

Inhibition of water transport was performed using mercury chloride ( $\text{HgCl}_2$ ), which is a known inhibitor of aquaporins (Maurel et al., 1997). Transformants were incubated with  $\text{HgCl}_2$  at 0.25, 0.5 and 1.0 mM for 15 and 30 minutes before the osmotic shock. Signals obtained were then compared with previous ones.

To evaluate if the regulation of this water channels is related to phosphorylation, glucose (100mM) was used instead of the hyperosmotic shock of 2.1M sorbitol.

In order to evaluate the effect of pH on aquaporin activity, adjustments of intracellular pH ( $\text{pH}_{\text{in}}$ ) experiments were undertaken by varying extracellular pH ( $\text{pH}_{\text{out}}$ ) and by adding benzoic acid, which promotes intracellular acidification due to the passive diffusion of the non-dissociated form of the acid followed by dissociation inside the cell. Cells were washed and incubated under three distinct conditions:  $\text{pH}_{\text{out}}$  6.8,  $\text{pH}_{\text{out}}$  5, and  $\text{pH}_{\text{out}}$  5 plus 4 mM benzoic acid in ice cold 1.4M sorbitol.

## 2.6 Growth assays under osmotic stress and sensitivity tests on atypical substrates

### Drop-tests

*S. cerevisiae* strains having *Quercus suber* aquaporins were tested for their ability to grow under osmotic stress. Moreover, their involvement in transport of atypical substrates such as

boron, hydrogen peroxide (H<sub>2</sub>O<sub>2</sub>) and arsenium was also investigated. Growth assays were performed on solid YNB medium (pH 5.0) supplemented with 2% (w/v) glucose and required substrates for the auxotrophies. Sorbitol (0.84, 1.4 and 2.1 M) was added to growth media for osmotic stress experiments. Hydrogen peroxide (0.5, 0.75 and 1mM), boron (as boric acid, 20, 40, and 60 mM), arsenate (0.2mM, 0.4mM and 0.8mM) and arsenite (0.5mM, 1.0 mM and 1.5mM), were used as atypical substrates for transport.

The evaluation of sensitivity/tolerance to osmotic stress and transport of unconventional solutes was carried out through drop-tests. For that, yeast strains expressing *Quercus* aquaporins were grown in liquid YNB medium supplemented with glucose and auxotrophic supplements until OD<sub>640nm</sub> 0.7-0.8 (beginning of exponential phase) (Ultrospec 2100 pro, Amersham Biosciences). Equal amount of cells were centrifuged (Eppendorf, Centrifuge 5870R) and resuspended in sterile distilled water and serial dilutions were made up to 10<sup>-7</sup> in 96 well plates. Then cells were stamped in drops of 3µl with the aid of the stamp (R2383 SIGMA) on YNB with 2% glucose and supplements for the auxotrophies, supplemented with desired test solutes. All of the plates were incubated at 28°C and the differences in the phenotype were recorded after 4 days, one week and two weeks.

### Growth curves

To confirm the results obtained in solid media and to evaluate the growth of the yeast cells, liquid media growth curves were performed. For that, liquid YNB medium (pH 5.0) supplemented with 2% (w/v) glucose and the supplements required for their auxotrophies was used. Sorbitol (2.1 M) was added to growth media for osmotic stress experiment. Hydrogen peroxide (0.25 mM) and boron (as boric acid 40mM) were chosen as atypical substrates. Yeast strains expressing *Quercus* aquaporins were grown in liquid media up to OD<sub>640nm</sub> 1.0 and inoculated in the YNB media supplemented with above mentioned test solutes at initial OD<sub>640nm</sub> 0.1. Cells were incubated at 28°C with 180rpm rotation. Cellular growth was evaluated by taking OD at 640nm every hour. The obtained values were then fitted on DMfit to estimate, specific growth rate, lag phase and final biomass using the model Baranyi and Roberts (Baranyi & Roberts, 1994). Graphics were then created to illustrate the growth of the cells.

### 2.7 Statistical analysis

For stopped-flow experiments, usually five runs at each temperature and ten runs for *Pf* at 23°C were stored and analyzed in each experiment. Student's t test was used for statistical analysis. P<0.05 was considered to be statistically significant. Levels of confidence are represented as P<0.05=\*, P<0.01=\*\* and P<0.001=\*\*\*. Data are presented as mean ± standard deviation (SD).

### 3. Results

#### 3.1 Cloning, sequence analysis and heterologous expression of *Q. suber* L. aquaporins in *aqy-null* *S. cerevisiae*

##### 3.1.1 PCR and cloning

The screening PCR with designed specific primers for *PIP2;4* and *TIP2;1* showed that cDNAs A1, A2, A5, HL2, HL4 and HL5 had amplification of QsTIP2;1 aquaporin of size 744 bp (Figure 3.1A), on the other hand all cDNAs had amplification of QsPIP2;4 aquaporin of size 804 bp (Figure 3.1B) revealing their expression in the correspondent tissues.

HL5 cDNA was chosen for *PIP2;4*, while HL2 cDNA was chosen for *TIP2;1* amplification, in order to obtain larger amount of amplicon. After the second PCR, enough PCR product of *PIP2;4* (1300ng) and of *TIP2;1* (500ng) was obtained to proceed further. These PCR products were gel-purified in order to remove carry-over primers and other impurities that can influence the cloning steps. After digestion with XbaI/SalI, PCR products and plasmid were purified, thereafter they were ligated using different vector: insert ratio. The product of ligation was transformed in *E. coli* with different ratios. All the used ligation ratios had separated colonies.

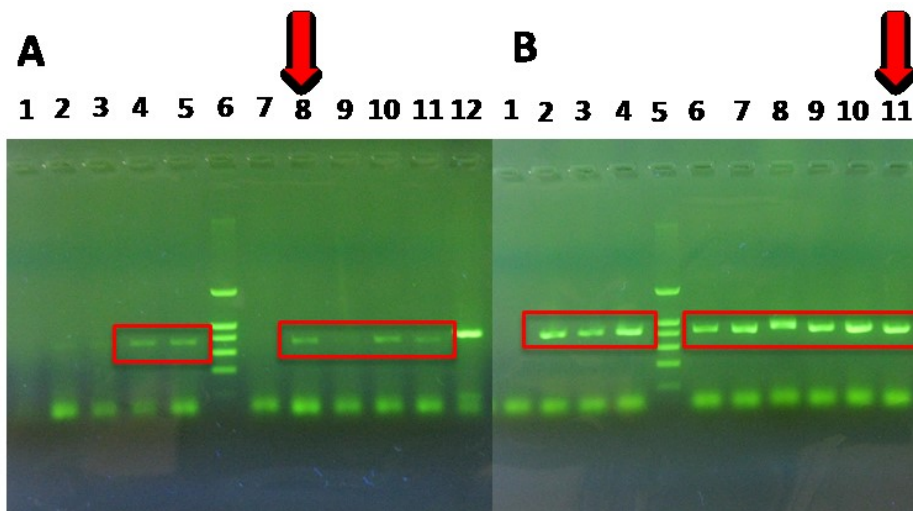


Figure 3.1 - PCR amplification with various cDNAs of *Q. suber* L. for amplification of *TIP2;1* (A) and *PIP2;4* (B). Picture A: 1 – negative control; 2 – G1; 3 – G2 ; 4 – A1; 5 – A2; 6 – ladder I; 7 – A5; 8 – HL2; 9 – HL3; 10 – HL4; 11 – HL5; 12 – positive control. Picture B: 1 – negative control; 2 – G1; 3 – G2 ; 4 – A1; 5 – ladder I; 6 – A2; 7 – A5; 8 – HL2; 9 – HL3; 10 – HL4; 11 – HL5. Arrows indicate the chosen cDNAs to proceed for further analysis.

##### 3.1.2 Insert analysis

After transformation, insert analysis was performed with at least three clones from each tried ligation ratio comparing the size of the plasmid with insert with the size of the empty vector. The clones that have acquired the insert should be larger than the empty one, hence they should move slower. This means that the plasmids that are above the band of control are likely to have

insert. According to this hypothesis, the clones showing higher molecular weight plasmids on the gel as compared to empty plasmid, were assumed to have the amplicon, and were selected for further clone analysis.

Clones A2, B2, C1, C4, E1 and F1 were chosen for *TIP2;1* and clones A1, A2, B2, B3, C1, D3, D4 and E3 were chosen for *PIP2;4* to continue with the clone analysis (Figure 3.2A and 3.2B, respectively). For that, plasmid was extracted and digested with *Xba*I and *Sal*I, and a PCR reaction was also performed using primers for pUG35 for the flanking region the amplicons. All selected clones were confirmed to have the desired insert (Figure 3.3).

After the confirmation of transformants with desired amplicon, at least 3 clones were selected to isolate the plasmid from kit and sent for sequencing.

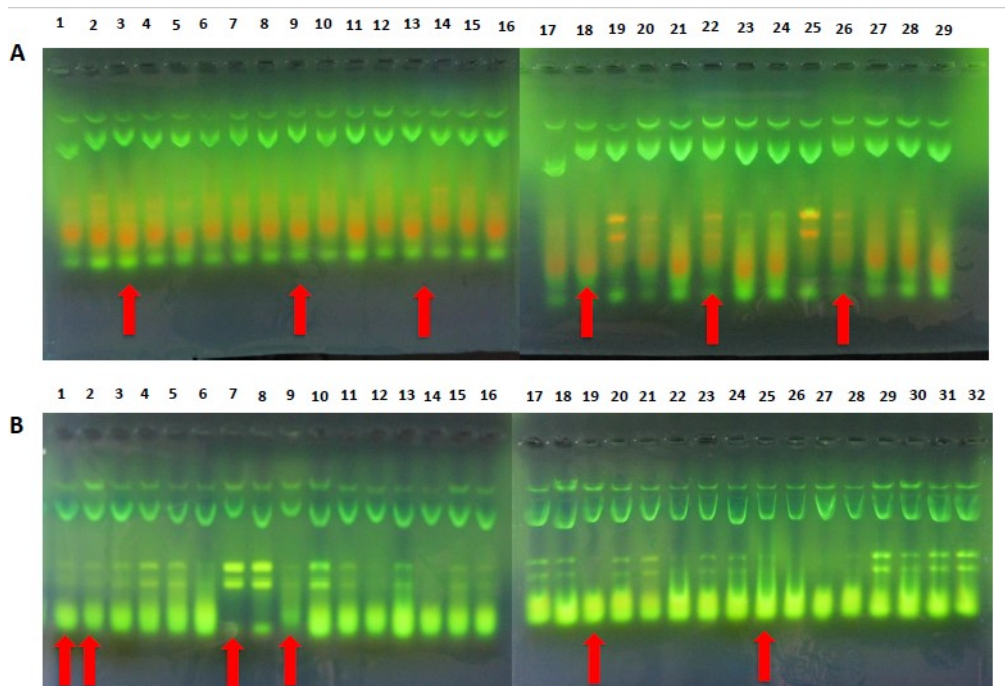


Figure 3.2 - Insert analysis of *Q. suber* L. *TIP 2;1* (A) and *PIP 2;4* (B). **A** - Lane 1: Religation, Lane 2: A1, Lane 3: A2, Lane 4: A3, Lane 5: A4, Lane 6: A5, Lane 7: B1, Lane 8: Religation, Lane 9: B2, Lane 10: B3, Lane 11: B4, Lane 12: B5, Lane 13: C1, Lane 14 : C2, Lane 15: C3, Lane 16: Religation, Lane 17: Religation, Lane 18: C4, Lane 19: D1, Lane 20: D2, Lane 21: D3, Lane 22:E1, Lane 23: Religation, Lane 24: E2, Lane 25: E3, Lane 26: F1, Lane 27: F2, Lane 28: F3, Lane 29: Religation. **B** - Lane 1: Clone A1; Lane 2 - Clone A2; Lane 3 - A3; Lane 4: A4; Lane 5 - A5; Lane 6 - B1; Lane 7 - B2; Lane 8: Religation; Lane 9 - B3; Lane 10 - B4; Lane 11 - B5; Lane 12 - C1; Lane 13 - C2; Lane 14 - C3; Lane 15 - C4; Lane 16 - C5; Lane 17 - D1; Lane 18 - D2; Lane 19 - D3; Lane 20 - D4; Lane 21 - D5; Lane 22 - E1; Lane 23 - E2; Lane 24 - Religation; Lane 25 - E3; Lane 26 - E4; Lane 27 - E5; Lane 28 - F1; Lane 29 - F2; Lane 30 - F3; Lane 31 - F4; Lane 32 - F5. Arrows indicate the clones chosen for following clone analysis.

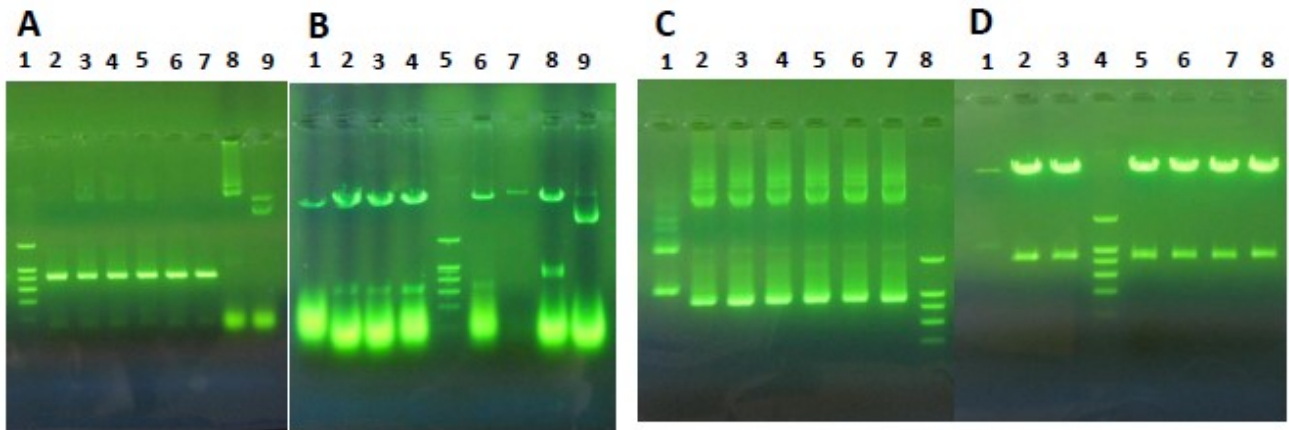


Figure 3.3 - Clone analysis of TIP2;1 clones by PCR (A) and by digestion (B) and Clone analysis of PIP 2;4 clones by PCR (C) and by digestion (D). (A) and (B): Lane 1 – Ladder; Lane 2 – Clone A2; Lane 3 – Clone B2; Lane 4 – Clone C1; Lane 5 – Clone C4; Lane 6 – Clone E1; Lane 7 – Clone F1; Lane 8 – Positive Control And Lane 9 – Negative Control. (C): Lane 1 – Positive Control; Lane 2 – Clone A1; Lane 3 – Clone A2; Lane 4 – Clone B2; Lane 5 – Clone B3; Lane 6 – Clone D3; Lane 7 – Clone E3 And Lane 8 – Ladder. (D): Lane 1 – Positive Control; Lane 2 – Clone A1; Lane 3 – Clone A2; Lane 4 – Ladder; Lane 5 – Clone B2; Lane 6 – Clone B3; Lane 7 – Clone D3; Lane 8 – Clone E3.

Sequences were compared using Blast tool revealing that all sequenced plasmids contained the correspondent aquaporin gene.

### 3.1.3 Heterologous expression in *aqy-null Saccharomyces cerevisiae*

Plasmids isolated from selected *E.coli* clones were used to transform *S. cerevisiae aqy-null*. To confirm the correct transformation and location of the obtained clones, yeast transformants were observed by fluorescence microscopy. As control, the *aqy-null* yeast strain transformed with the empty plasmid was used.

As expected, when the clones were observed in the microscope it was found that empty plasmid had fluorescence in cytosol and the chosen transformants, either with QsTIP2;1 or QsPIP2;4 showed fluorescence in the yeast membrane (figure 3.4). Indicating their correct localization and sorting to the membrane.



### 3.1.5 Topology prediction

In order to predict topology and the localization of the aquaporins detected, the deduced amino acid sequences were analyzed through Topology Prediction tools of ExPASy.

All deduced amino acid sequences of QsPIP2;4 and QsTIP2;1 exhibited characteristic feature of typical aquaporins.

- 1) 6 transmembrane helices,
- 2) 5 loops and cytosolic N- and C-termini.

The same was not observed for the database sequence of PIP2;4 that showed only 5 transmembrane helices and four loops, suggesting that it does not correspond to a complete sequence.

Besides the general characteristics, some family specific features were also found, such as a His residue for pH sensitivity in QsPIP2;4 (position 193), and a Ser residue at C-terminal in the consensus phosphorylation site (Lys-x-xx-Ser-x-Arg) which is conserved only in PIP2 subfamily was also found (position 274) (Figures 3.6 and 3.7).



Figure 3.6 - Weblogo image displaying the conserved Histidine in position 193. For this analysis 44 sequences were used. Accession numbers of the sequences used: POE96352, POE66465, POE97127, XP\_023923839, XP\_023923152, XP\_023870587, POF11915, XP\_023926845, XP\_023926844, XP\_023887849, XP\_023899033, CAO41326, CAO62835, CAO39626, CAO41326, CAN75442, CAO47394, CAO18152, CAO21844, KJ697714, KJ697715, KJ697716, P61837, Q06611, Q08733, Q39196, Q8LAA6, P43286, P43287, P30302, Q9FF53, Q9SV31, Q9ZV07, P93004, Q9ZVX8, AFH36339, AFH36340, AFH36341, AFH36336, AFH36337, AFH36338, ACV70047, ACV70053, ACV70055.



Figure 3.7 - Weblogo image displaying the conserved Serine in position 274. In this analysis 24 sequences were used. Accession numbers of the sequences used: POF11915, XP\_023926845, XP\_023926844, XP\_023887849, XP\_023899033, POE92575, XP\_023899033, CAN75442, CAO47394, CAO18152, CAO21844, KJ697715, KJ697716, P43286, P43287, P30302, Q9FF53, Q9SV31, Q9ZV07, P93004, Q9ZVX8, AFH36336, AFH36337, AFH36338.

For QsTIP2;1, a Cys residue associated with mercury sensitivity was found (position 116) (Figure 3.8), a Thr residue which is a putative phosphorylation site (position 97) (Figure 3.9) and a His residue related with pH sensitivity (position 131) (Figure 3.10).

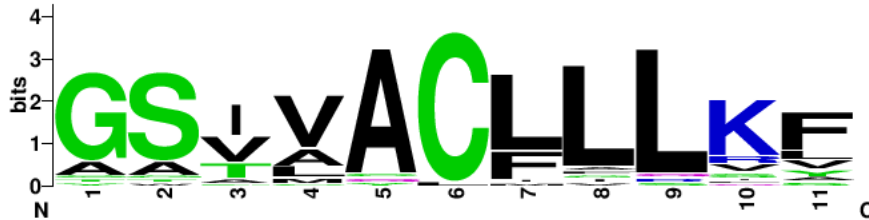


Figure 3.8 - Weblogo image displaying the conserved Serine in position 274. In this analysis 30 sequences were used. Accession numbers of the sequences used: POE65492, XP\_023920799, XP\_023904770, POE73559, XP\_023903922, POF05546, POE96780, CAO69259, CAO63006, CAO16745, CAO21720, CAO23095, CAO44039, CAO42713, CAO70596, KJ697717, HQ913640, P25818, Q41963, O82598, Q41951, Q41975, Q9FGL2, P26587, O22588, O82316, Q9STX9, AFH36342, AFH36343, AFH36344.

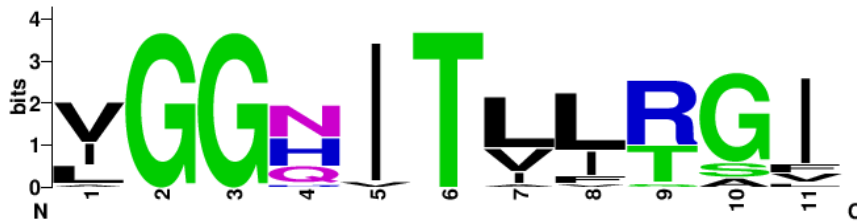


Figure 3.9 - Weblogo image displaying the conserved Threonine in position 97. In this analysis 21 sequences were used. Accession numbers of the sequences used: POE65492, XP\_023920799, POE73559, XP\_023903922, POE96780, CAO69259, CAO63006, CAO16745, CAO21720, CAO45860, CAO23095, CAO44039, KJ697717, HQ913640, P25818, Q41963, O82598, Q41951, Q41975, Q9FGL2, P26587, AFH36343, AFH36344.

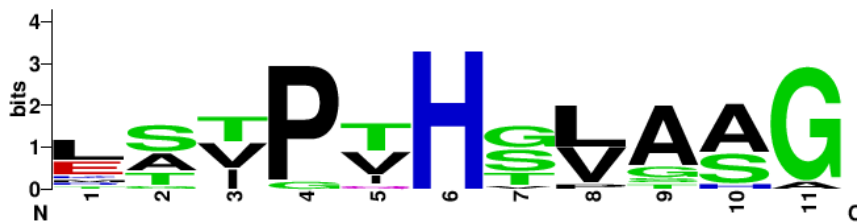


Figure 3.10 - Weblogo image displaying the conserved Histidine in position 131. Accession numbers of the sequences used: XP\_023903922, POF05546, CAO45860, CAO23095, CAO44039, CAO42713, HQ913640, Q41951, Q41975, Q9FGL2, O82316, AFH36342, AFH36343.

### 3.1.6 Signature sequence for atypical substrates

Sequences were analyzed for signature residues for atypical substrates, especially in the ar/R filter. This constriction filter is composed by four different residues, one located in the second (H2) and one in the fifth helix (H5) and two in the fifth loop (Loop E), all of them presented signature elements for boron and H<sub>2</sub>O<sub>2</sub>. For boron, residues found were F on the TMH2, H on TMH5, and T and R in Loop E (Figure 3.11).

		TMH2 (ar/R)	TMH5 (ar/R)	Loop E(1) (ar/R)	Loop E(2)(ar/R)
PIP group	VvTnPIP 1;4	IAWAF	FLVHLA	TGTGIN	NPARSL
	VvTnPIP 2;1	IAWSF	FMVHLA	TGTGIN	NPARSL
TIP group	VvTnPIP 2;3	IAWAF	FMVHLA	TGTGIN	NPARSL
	AtPIP 2;4	IAWAF	FMVHLA	TGTGIN	NPARSF
	→ QS_PIP24_A2	IAWAF	FMVHLA	TGTGIN	NPARSF
	→ QSPIP24_B2	IAWAF	FMVHLA	TGTGIN	NPARSF
	VvTnTIP 2;1	VAVAH	GANILA	SGGSMN	NPARSF
	VvTnTIP 1:1	AALAH	GANILA	DGASMN	NPAVSF
	AtTIP 2;1	IAVCH	GANILA	SGGSMN	NPARSF
	→ QsTIP 2.1	IAICH	GANILA	SGGSMN	NPARSF

Figure 3.11 - Signature sequences for atypical substrates, boron and hydrogen peroxide. Arrows identify the sequences obtained in this study.

### 3.1.7 Phylogenetic analysis

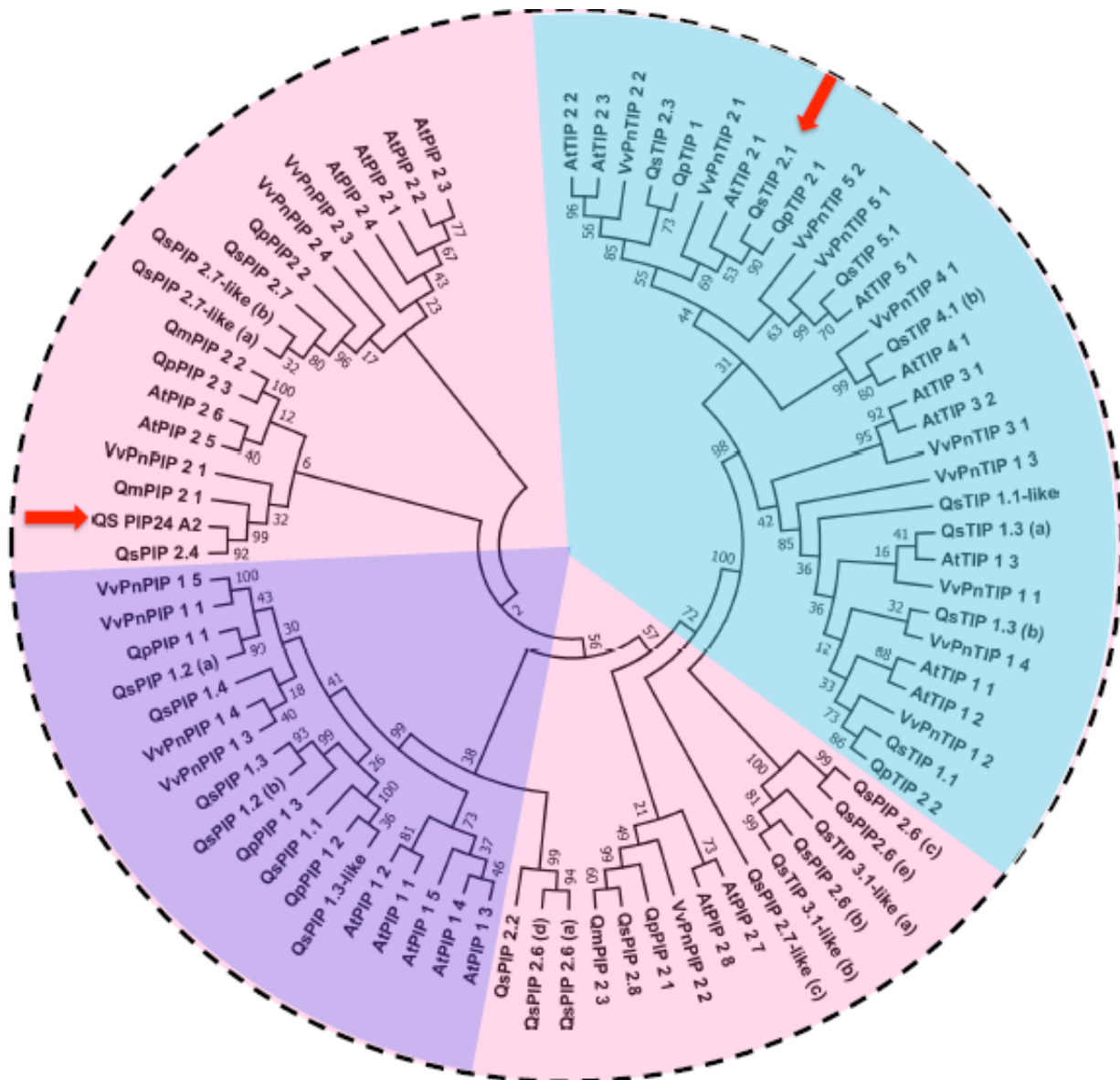


Figure 3.12 - Phylogenetic tree obtained with Neighbor-Joining method, bootstrap and 1000 replicates. Arrows point to the sequences obtained in this study. Accession numbers of the used sequences: POE65492, XP\_023920799, XP\_023904770, POE73559, XP\_023903922, POF05546, XP\_023889965, XP\_023889944, POE96780, XP\_023917997, POE96352, XP\_023888245, POE66465, XP\_023923839, XP\_023923152, XP\_023870587, POE77117, POF11915, XP\_023919491, POF21789, POF21792, POF01595, XP\_023926844, XP\_023887849, POE92575, XP\_023899033, AFH36339, AFH36340, AFH36341, AFH36336, AFH36337, AFH36338, AFH36342, AFH36344, ACV70039, ACV70047, ACV70053, CAO41326, CAO62835, CAO39626, CAO41326, CAN75442, CAO47394, CAO18152, CAO21844, CAO69259, CAO63006, CAO16745, CAO21720, CAO45860, CAO23095, CAO62035, CAO44039, CAO42713, CAO70596, P61837, P61837, Q08733, Q39196, Q8LAA6, P43286, P43287, P30302, Q9FF53, Q9SV31, Q9ZV07, P93004, Q9ZVX8, P25818, Q41963, O82598, Q41951, Q41975, Q9FGL2, P26587, O22588, O82316, Q9STX9.

As it can be observed in the image, there are three well defined clusters, one for TIP group, marked in blue, one for PIP1, marked in purple, and another for PIP2, marked in pink. PIP2 group, however, has its members divided.

### 3.2. Water transport activity

Water permeability was assessed by stopped-flow fluorescence spectroscopy. The shrinking rate of yeast cells due to applied sorbitol hyperosmotic shock was evaluated as a change in fluorescence intensity. The strain harboring the empty plasmid pUG35 was used as a control as it doesn't have any native *aqy* channel.

The QsPIP 2;4 B presented a mean  $P_f$  of  $4.05 \pm 0.27 \times 10^{-4} \text{ cm}^{-1}$ , which is not significantly lower than the  $P_f$  value obtained for the cells with the pUG35 vector, which means that the water permeability was not affected by the presence of this particular water channel and was not functional in the tested conditions. However, QsPIP 2;4 A and especially QsTIP 2;1 showed higher permeability (mean  $P_f$  value of QsTIP2;1 is  $13.41 \pm 0.37 \times 10^{-4} \text{ cm}^{-1}$  and QsPIP2;4 A is  $6.22 \pm 0.59 \times 10^{-4} \text{ cm}^{-1}$ ) and were considered as functional aquaporins (Figure 3.13).

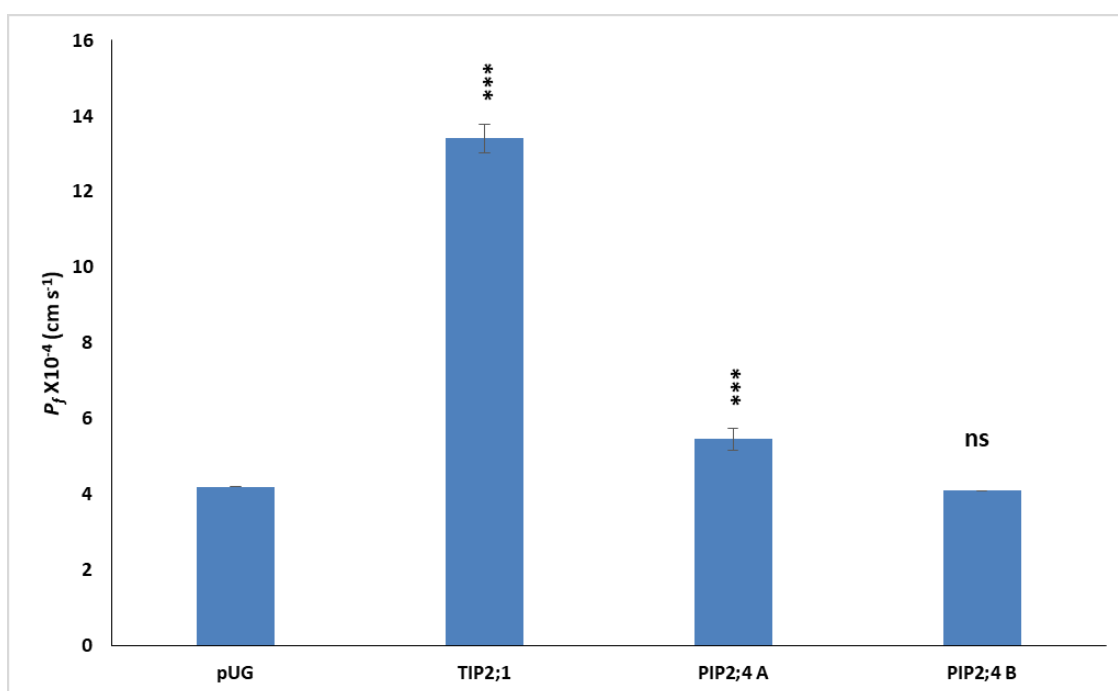


Figure 3.13 - Water permeability coefficients ( $P_f$  at 23°C) of QsTIP 2;1 and QsPIP2;4 A were higher. Expression of QsPIP2;4 B did not increase water permeability in yeast cells. Data are mean  $\pm$  SD of three independent experiments.

The activation energy for water transport was evaluated through the analysis of  $P_f$  values in a range of temperatures (9 to 33°C) and Arrhenius plots were created. As expected, the permeability was highly dependent on temperature in cells expressing empty plasmid and non-functional aquaporin, as reflected by higher activation energies ( $E_a$  (kcal mol<sup>-1</sup>) of empty pUG35 is 13.56 kcal mol<sup>-1</sup>). For the strains expressing functional aquaporins, water permeability were not much affected by temperature with lower activation energies ( $E_a$  (kcal mol<sup>-1</sup>) of QsTIP2;1

(7.30 kcal mol<sup>-1</sup>) and QsPIP2;4 A (11.47 kcal mol<sup>-1</sup>), suggesting that the water is passing by the aquaporins (Figure 3.14).

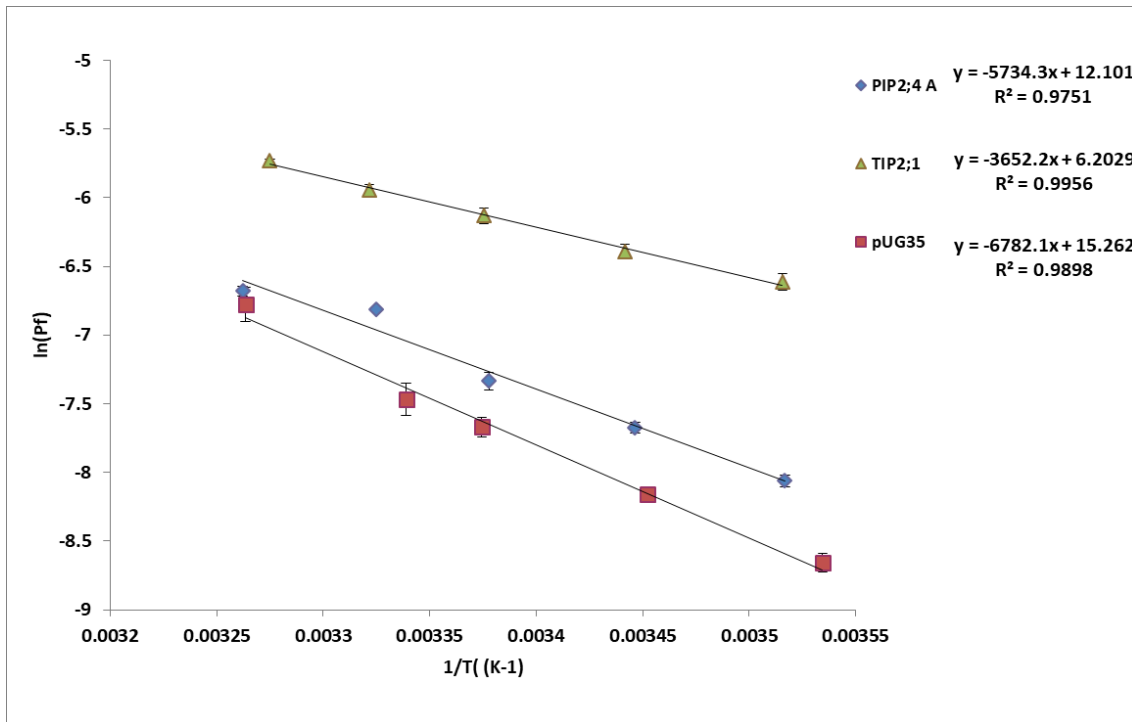


Figure 3.14 - Arrhenius plot of Pf at temperature range (11–34°C), where T is temperature in Kelvin. Ea was evaluated from the slopes. Empty plasmid (pUG35) showed steeper slope, while strains expressing QsTIP2;1 and Qs PIP2;4 A exhibited shallow slope.

Since mercury chloride (HgCl<sub>2</sub>) is considered as an inhibitor for aquaporins (Maurel et al., 2008), the effect of 0.5mM HgCl<sub>2</sub> was evaluated by incubating the cells for 15 minutes at room temperature before the hyperosmotic shock. QsTIP2;1 expressing strain showed a slight reduction of the water permeability. On the contrary, QsPIP2;4A expressing strain exhibited an increase in water permeability in the presence of mercury chloride (Figure 3.15).

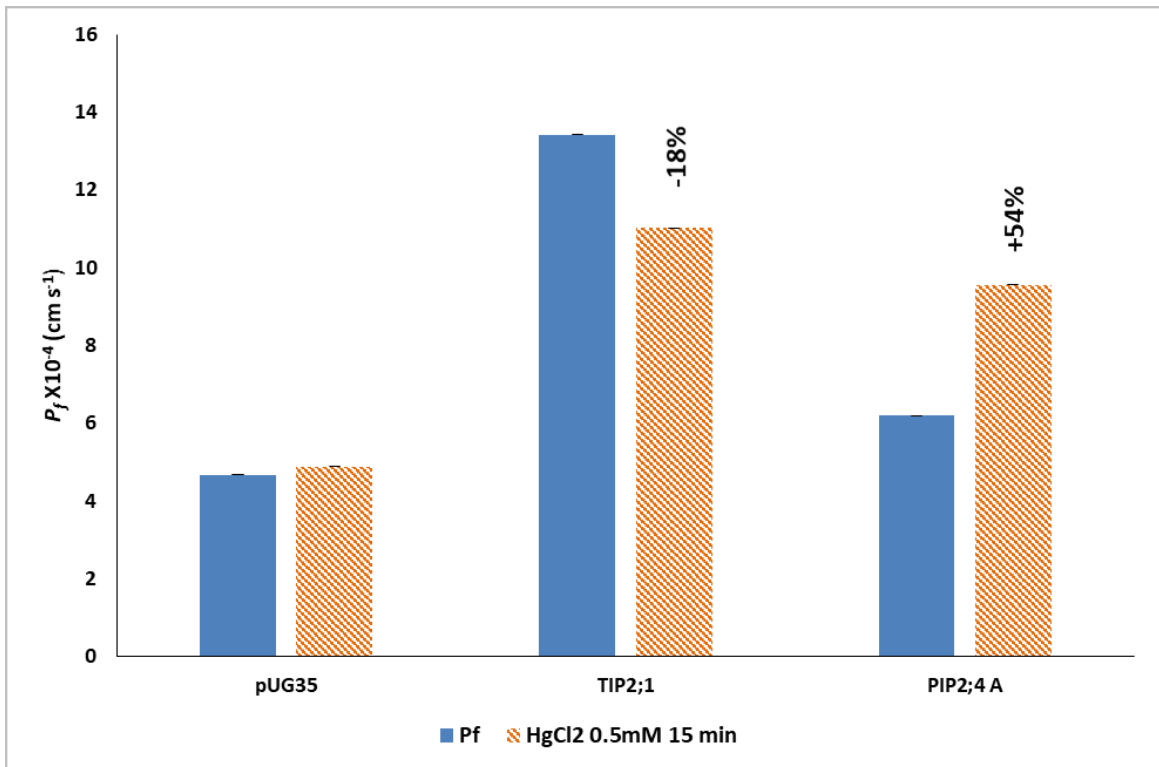


Figure 3.15- Water permeability coefficients ( $P_f$  at 23°C) of QsTIP2;1 was reduced by 0.5mM of Mercury chloride, while QsPIP2;4 A increased. Data are mean  $\pm$  6 SD of two independent experiments.

When  $\beta$ -mercaptoethanol was added to the cells, the effect of mercury chloride was reversed by 14% (Figure 3.16).

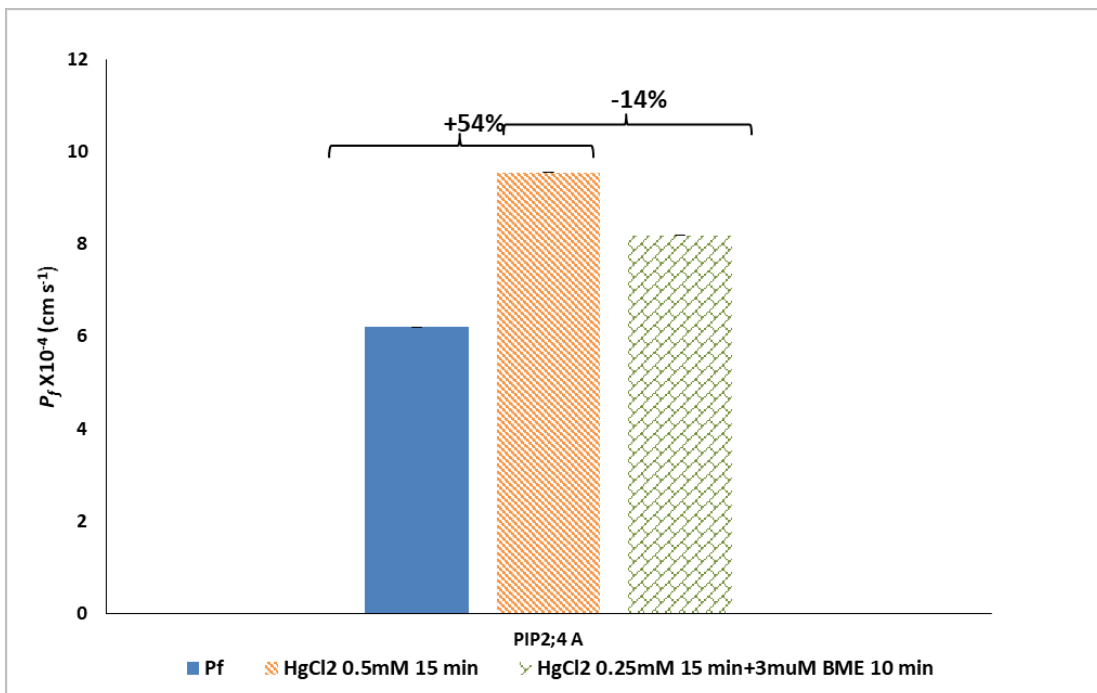


Figure 3.16 - Water permeability of QsPIP2;4A in the presence of mercury and BME

It has been proved that cAMP regulates some aquaporins' expression through a protein kinase A (PKA) pathway (Yang, Kawedia, & Menon, 2003). In yeast, the basal intracellular cAMP concentration is low but by adding glucose after starvation, it triggers the Ras/PKA pathway. This pathway increases the intracellular concentration of cAMP leading to a phosphorylation cascade (Mbonyi, Aelst, Arguelles, Jans, & Thevelein, 1990; Rodrigues et al., 2016). To evaluate if Quercus aquaporins are regulated by phosphorylation, a glucose shock was subjected to glucose starving yeast cells prior to  $P_f$  measurement at pH 5.0. We found that glucose shock did not affect the water permeability of the yeast strains. A slight reduction was observed in all strains including the empty plasmid expressing strain, suggesting a general effect of glucose addition (Figure 3.17).

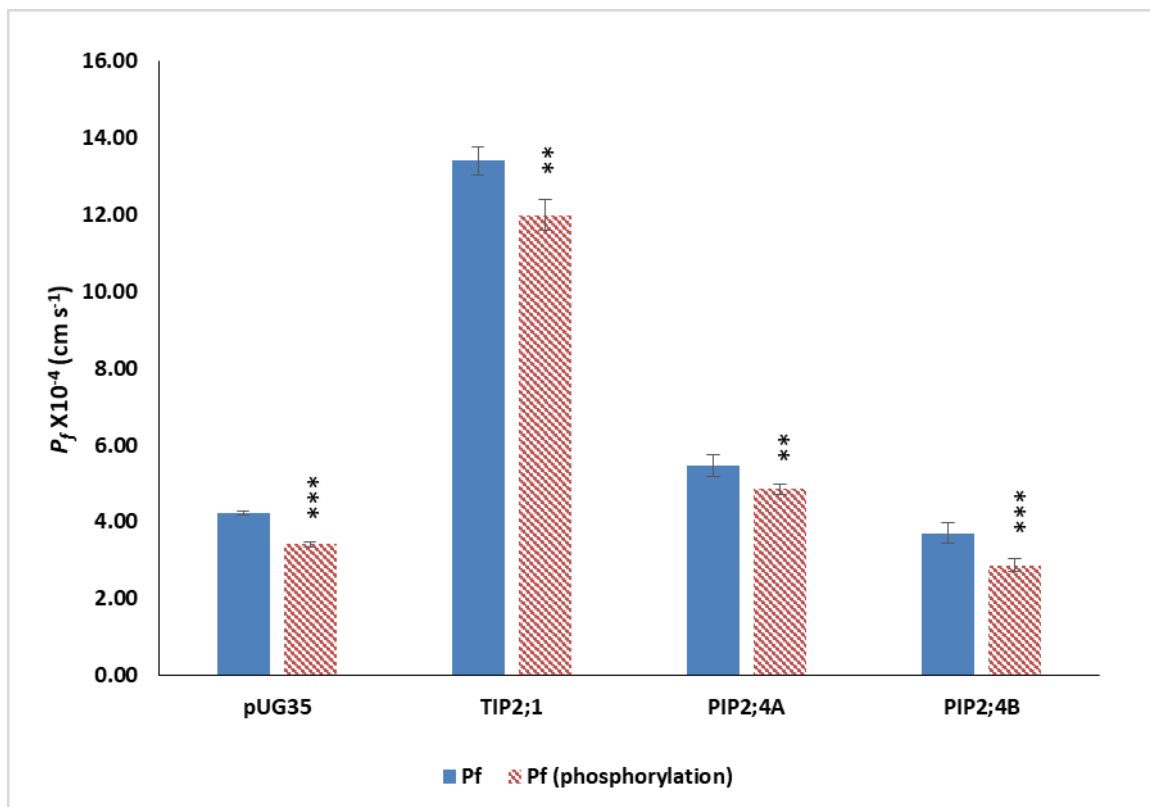


Figure 3.17 - Phosphorylation effect on QsTIP2;1 QsPIP2;4 A and QsPIP2;4 B.  $P_f$  value at pH 5.0 slightly reduced the water permeability of all Quercus suber L. and empty plasmid.

Since there is evidence of aquaporins being regulated by pH (Tournaire-Roux C, Sutka M, Javot H, Gout E, 2003), pH effect on aquaporin activity was evaluated. For that, yeast cells expressing Q. suber aquaporins were analyzed by varying extracellular pH (pH<sub>out</sub>) and by adding benzoic acid, which promotes intracellular acidification due to the passive diffusion of the non-dissociated form of the acid followed by dissociation inside the cell (Leitão et al., 2012). In what concerns the pH effect, it was observed that intracellular acidification didn't led to changes in the  $P_f$  values but pH 6.8 increased permeability in all strains (Figure 3.18), except control. QsTIP2;1 value increased from  $13.41 \pm 0.37 \times 10^{-4} \text{ cm}^{-1}$  to  $20.60 \pm 0.93 \times 10^{-4} \text{ cm}^{-1}$  (52%), QsPIP2;4

A value changed from  $6.22 \pm 0.59 \times 10^{-4} \text{ cm}^{-1}$  to  $12.28 \pm 0.52 \times 10^{-4} \text{ cm}^{-1}$  (98%) and an increase in  $P_f$  of QsPIP2;4 B was also changed from  $3.70 \pm 0.27 \times 10^{-4} \text{ cm}^{-1}$  to  $6.33 \pm 0.24 \times 10^{-4} \text{ cm}^{-1}$  (66%).

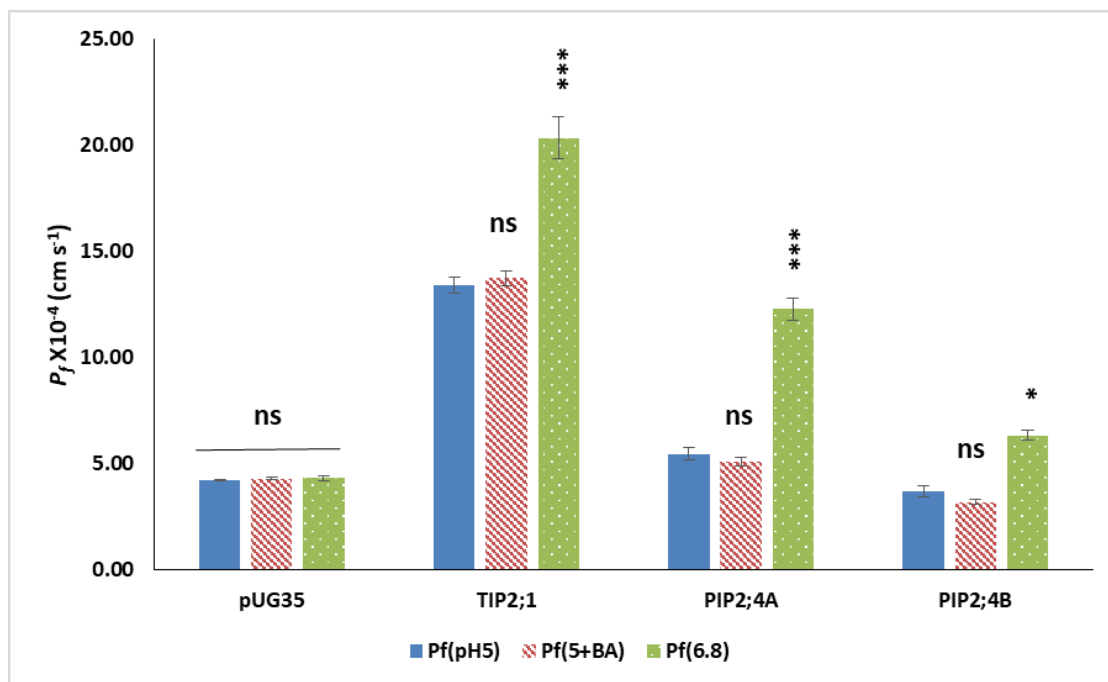


Figure 3.18 - Water permeability of yeast strains expressing QsTIP2;1, QsPIP2;4 A and QsPIP2;4 B. permeability coefficient ( $P_f$ ) was measured at intracellular pH 6.8, pH 5 and pH 5 + benzoic acid.

### 3.3 Growth assays

#### 3.3.1 Growth assays under osmotic stress and atypical substrates

To investigate the possibility of transport of atypical substrates through *Q. suber* aquaporins, and their role in osmotic tolerance, growth assays of yeast strains expressing *Q. suber* aquaporin were performed under either osmotic stress or in the presence of atypical substrates (figure 3.19).

As expected, after two weeks of incubation at 28°C, QsPIP2;4 B (which doesn't have functional aquaporin) manifests a similar phenotype to the control strain, except for boron transport in which it appears to be more sensitive. On the other hand, QsTIP2;1 and QsPIP2;4 A present sensitivity both to osmotic stress by 2.1M sorbitol and 0.5mM hydrogen peroxide, with QsTIP2;1 being more sensitive. This might indicate that both aquaporins may have a role in osmoregulation as well as role in transport of hydrogen peroxide.

In the presence of lower concentration of  $\text{H}_2\text{O}_2$  (0.5mM), QsTIP 2;1 strain was more sensitive, followed by QsPIP 2;4 A strain. The cells showed marked signs of ageing as the colonies look darker and bigger than control plates.

As for Boric Acid plates, it was possible to observe a high sensitivity of the three aquaporins tested at 40 mM concentration. In this case, PIP 2;4 B expressing strain was the most sensitive, followed by PIP 2;4 A and TIP 2:1 expressing strains.

In regard of arsenate (V) and arsenite (III), no phenotype was observed in any tested concentration (results not shown).

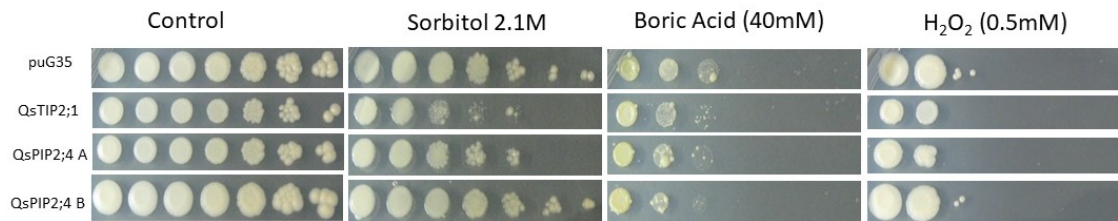


Figure 3.19 - Growth assays of *S. cerevisiae* strains expressing *Q. suber* aquaporins under osmotic stress and atypical substrates. Yeast strain transformed with empty pUG35 plasmid was used as control (pUG35). Yeast suspensions were spotted in 10-fold dilution on solid YNB plates with 2.1 M sorbitol. Growth was recorded after two weeks at 28°C.

### 3.3.2 Growth assays under osmotic stress and atypical substrates in liquid media

To confirm the results obtained in the drop tests, the growth of *S. cerevisiae* containing the cloned *Q. suber* aquaporins was performed. Based on the results from plates, the concentrations chosen for this assay were 2.1M sorbitol to exert osmotic stress and 40mM of Boric Acid to evaluate for boron transport. To observe the transport of hydrogen peroxide a lower concentration (0.25mM) was chosen because at 0.5mM the clones exhibited growth inhibition.

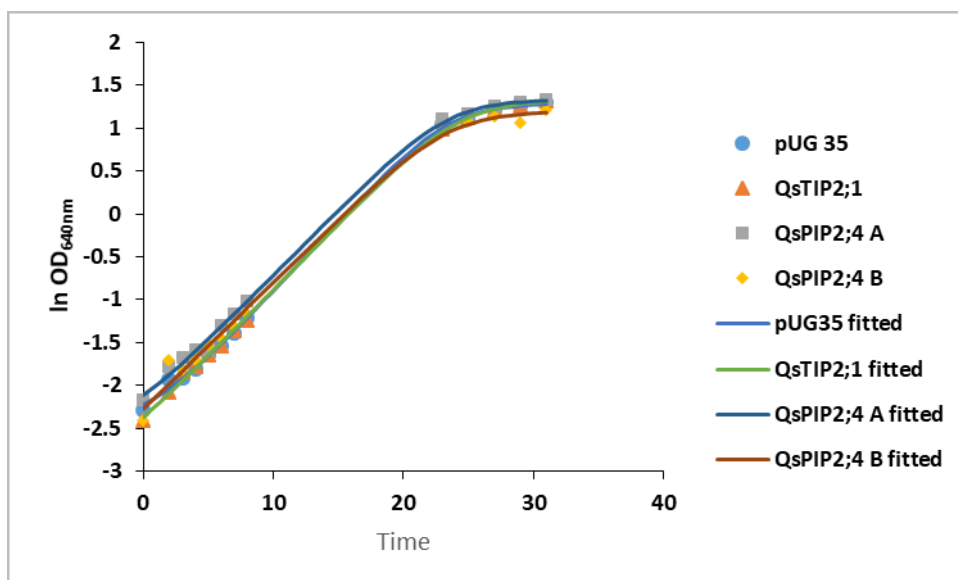


Figure 3.20 - Growth curve of all yeast strains on YNB+2% glucose+LTH (control conditions).

Under osmotic stress, duplication time and overall growth were not significantly different (Figure 3.21) but there is a slight difference in the final biomass of QsTIP2;1, which reached a lower value than its control (table 3.1).

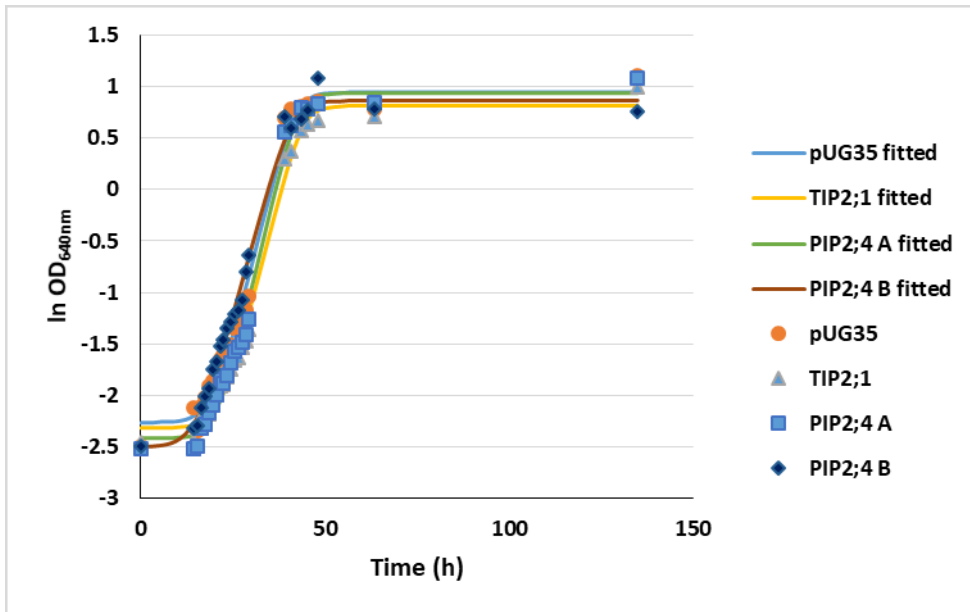


Figure 3.21 - Growth curve of all yeast strains on YNB+2% glucose+LTH and 2.1M sorbitol. This conditions were meant to evaluate the effect of the osmotic stress.

Strains grown in the presence of boric acid, on the other hand, exhibited differences in duplication time, QsTIP2;1 and QsPIP2;4 A showed a remarkable increase, although in terms of final biomass (Table 3.1), QsTIP2;1 showed lower growth (Figure 3.22).

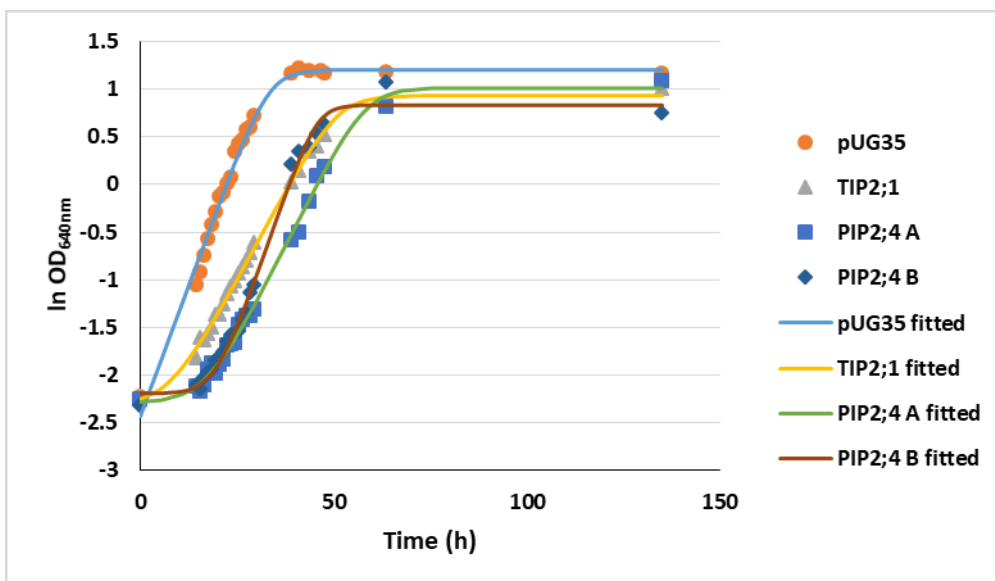


Figure 3.22 - Growth curve of all yeast strains on YNB+2% glucose+LTH and 40mM Boric acid. This conditions were applied to observe the transport of boron.

In what concerns hydrogen peroxide, it was possible to observe that the highest effect occurs on QsTIP2;1 (Figure 3.23). In this case, both duplication time and final biomass were highly affected by the presence of hydrogen peroxide, even at a lower concentration (0.25mM) (Table 3.1).

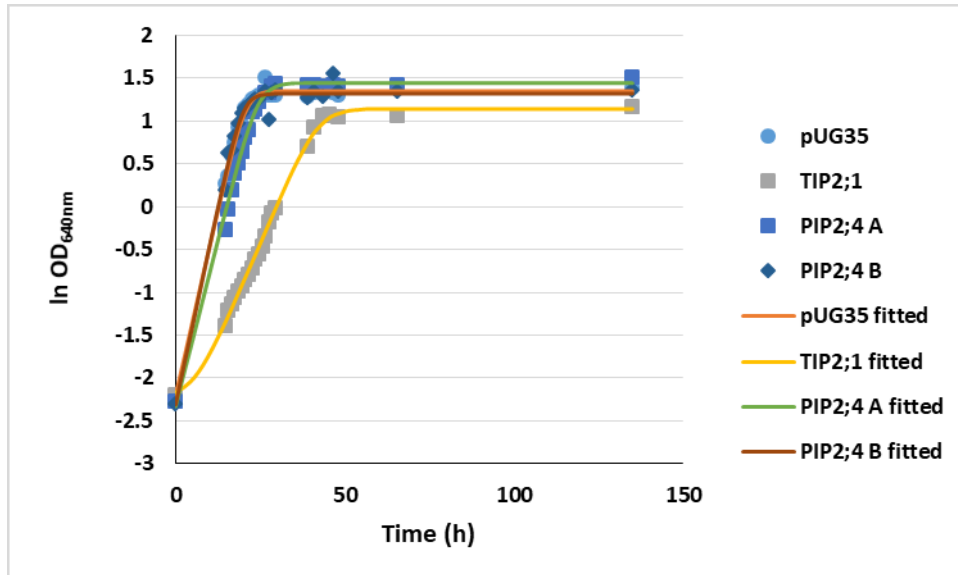


Figure 3.23 - Growth curve of all yeast strains on YNB+2% glucose+LTH and 0.25mM H<sub>2</sub>O<sub>2</sub>. This conditions were applied to observe the transport of hydrogen peroxide.

Table 3.1 - Growth parameters of QsTIP2;1, QsPIP2;4 A and QsPIP2;4 B obtained for growth in liquid media under osmotic stress and atypical substrates.

		Duplication time (h)	Final biomass
<b>YNB + 2% Glucose + LTH</b>	<i>pUG35</i>	4.47	1.286
	<i>QsTIP2;1</i>	4.56	1.329
	<i>QsPIP2;4 A</i>	4.6519945	1.331
	<i>QsPIP2;4 B</i>	4.747583428	1.192
<b>Sorbitol 2.1M</b>	<i>pUG35</i>	4.881318173	2.575387479
	<i>QsTIP2;1</i>	4.986670364	2.261435978
	<i>QsPIP2;4 A</i>	4.590378679	2.559981418
	<i>QsPIP2;4 B</i>	5.291199852	2.37738228
<b>Boric Acid 40mM</b>	<i>pUG35</i>	6.359148446	3.326763801
	<i>QsTIP2;1</i>	9.266673537	3.040433184
	<i>QsPIP2;4 A</i>	8.696953332	2.745875589
	<i>QsPIP2;4 B</i>	6.027366787	2.406082726
<b>H2O2 0.25mM</b>	<i>pUG35</i>	4.006631102	3.857425531
	<i>QsTIP2;1</i>	7.485390719	3.129896697
	<i>QsPIP2;4 A</i>	4.471917294	4.237612411
	<i>QsPIP2;4 B</i>	3.746741517	3.75842505

## 4. Discussion

In this study we have successfully cloned and characterized two aquaporins, one TIP and one PIP, from *Quercus suber*, one of the most important trees from the Portuguese montado (QsTIP2;1 and QsPIP2;4).

The full length aquaporin cloned genes from *Q. suber* encoding one PIP and one TIP showed similarities with the same proteins from the database. Although QsPIP2;4 was found to have extra nucleotides in the cloned sequence, this was considered as the accurate sequence, not the database one, because when they were evaluated topologically it was found that the database sequence didn't have the typical topology of an aquaporin. The localization of the proteins in the yeast plasma membrane was confirmed by GFP.

The phylogenetic analysis showed some very well defined clusters. However, the division of PIP2 group was not expected. Since there are three aquaporins with very well defined characteristics in the pink cluster between the PIP1s and the TIPs, it is to assume that they are correctly annotated and that the presence of this aquaporins separately from the others of the same group might mean that either the method used is too sensitive to differences or that they have evolved phylogenetically in a different manner. In the case of QsPIP2;6, QsPIP2;7 and QsPIP2;2, there is a strong probability of them not being correctly annotated since they appear to belong to clusters other than PIP2 group.

The expression of the cloned aquaporins QsPIP2;4 A and QsTIP2;1 increased the water permeability coefficient and reduced the activation energy, and they were considered as functional for water transport.

In what concerns QsPIP2;4 B, it was observed that the permeability coefficient was not significantly different than the value obtained for the empty plasmid, which means this is a non-functional aquaporin. Interestingly, the sequence analysis revealed that in QsPIP 2;4 Thr<sup>70</sup> was replaced by a Ser in B2 clone. With that in mind, we analyzed aquaporins from other species and found that, for those already studied regarding water transport, the aquaporins having a Thr in that same position were functional for water transport and the ones having a Ser were not. For example AtPIP2;5, AtTIP1;1, AtTIP1;2, AtTIP3;1 and AtTIP4;1 have a Thr at that position and were observed as functional (Bienert et al., 2007; Hofte et al., 1992; Ines, 2008; Liu, 2003; Maurel et al., 1993), same as VvTIP1;1 (Sabir et al., 2014). On the other hand, VvTnPIP1;1 and VvTnTIP4;1 have a Ser and they are considered as nonfunctional (Leitão et al., 2012; Sabir et al., 2014). Although we were unable to observe it, this might be due to phosphorylation, because these amino acids are known phosphorylation sites (Han, Wang, Chen, Dong, & Fan, 2017).

QsTIP2;1 exhibited much higher water conductivity in comparison to QsPIP2;4. This might be due to the fact that TIPs are vacuole specific aquaporins and may be needed for the osmotic regulation of the cytoplasm (Sabir et al., 2014).

In general, mercury chloride is considered as an inhibitor of aquaporin activity. Contrary to the expected, our results showed a marked increment in water permeability of QsPIP2;4A in the presence of mercury chloride. The same behavior has been observed for SoPIP2;1 (Frick et al., 2013).

Despite the numerous hypothesis concerning the way Mercury chloride works (Frick et al., 2013; Katsuhara et al., 2014), a more recent work suggests that the activation by mercury chloride might be by direct binding to the aquaporin (Kirscht et al., 2016). In fact, the analysis of our proteins showed that all the mentioned residues in SoPIP2;1 are also present in our sequence QsPIP2;4 (data not shown). Also, when QsPIP2;4 was aligned with OsNIP3;3, it was found that *Quercus suber* L. sequence also does not have an Histidine in position 168, which was thought to have influence in the OsNIP3;3 mercury activation (Katsuhara et al., 2014), so one could think this is not the residue causing the activation by mercury. However, further analysis are needed to understand what are the reasons behind this unusual mercury activation.

Phosphorylation has been reported as an important post-translational modification. As a matter of fact, PIP2s carry many conserved phosphorylation sites in *loop* B and C-terminal tail (Verdoucq, Rodrigues, Martinière, Luu, & Maurel, 2014). Actually, in SoPIP2;1, phosphorylation of Ser<sup>274</sup> in the C-terminal tail acts on an adjacent monomer and prevents its change into a closed-pore state, and, as mentioned before, a serine phosphorylation in loop B disrupts a connection between loop D and the N-terminal tail, causing the water channel to remain open (Verdoucq et al., 2014). Also in TIPs, it has been observed that its activity can be modulated by phosphorylation, activating the channel and allowing for the water to pass. In rat AQP-5, phosphorylation has been proved to have a significant role in the gating and regulation (Rodrigues et al., 2016). The aquaporins evaluated in this study have putative phosphorylation sites. However, no effect on water permeability was observed due to addition of glucose at pH 5.0. Similarly, water permeability of rat AQP-5 expressing yeast strain was unaffected by glucose shock but an increase in the permeability at higher pH (pH 7.4) was observed (Rodrigues et al., 2016). Further assays are required to ascertain the role of the serine and threonine residues as phosphorylation sites in aquaporin.

Water permeability of *Quercus suber* aquaporins were unaffected by lower internal pH (4.5), caused by benzoic acid. On the other hand, at higher external pH (6.8), an overall increased water permeability was observed. Even the permeability of non-functional QsPIP2;4 B was also increased due to extracellular higher pH. Our results are not in line to the findings which demonstrated that some plant aquaporins gating are regulated by intracellular acidification

(Leitão et al., 2012). Studies suggest the Histidine residue in *loop D* as pH sensor in plant aquaporins, despite having this conserved residue in *Quercus* aquaporins, intracellular pH alteration did not affect their water permeability (Fischer & Kaldenhoff, 2008; Törnroth-Horsefield et al., 2006; Tournaire-Roux C, Sutka M, Javot H, Gout E, 2003). Furthermore, it was proposed that although this Histidine residue is a major pH sensing-site, it's not the sole residue responsible for pH dependent gating of aquaporins (François Chaumont et al., 2005). Our results indicate that the observed higher permeability in higher extracellular pH of PIP2;4B expressing strain, which was observed to be non-functional for water transport at pH 5.0 due to the change of single amino acid T70S, may be due to changes in the conformation of protein from closed to open state. Besides, this aquaporin expressing strain showed putative involvement in transport of other atypical substrates, suggesting that its functional involvement in membrane transport cannot be excluded.

Contrary to the plant aquaporins, animal aquaporins have been suggested to be regulated by extracellular pH (Almeida et al., 2016). Recently, A. Mosca and co-workers have reported that AQP-7 is regulated by pH, changing from permeable to almost fully closed at acidic pH, and that the residues Tyr<sup>135</sup> and His<sup>165</sup> are crucial for the channel permeability (Mósca et al., 2018).

In what concerns the transport of atypical substrates, the topology prediction of the two cloned aquaporins showed the specific residues for boron and hydrogen peroxide in the ar/R constriction filter. All cloned *Q. suber* aquaporins were tested under H<sub>2</sub>O<sub>2</sub> and boric acid growth conditions to investigate their ability to transport these atypical substrates. The growth phenotype variations showed that heterologous expression of QsTIP2;1 caused more susceptibility to externally applied H<sub>2</sub>O<sub>2</sub>, indicating their putative role in the transport of this toxic compound. An increased level of hydrogen peroxide can disturb the cellular metabolism in an unidentified manner, which may lead to reduced or impaired growth of yeast cells (Sabir et al., 2014). In fact, hydrogen peroxide causes yeast clones to get larger and fluffier, which might be due to cell ageing caused by the release of reactive oxygen species. As for boron, an essential micronutrient required in all higher plant's, the susceptibility tests to higher concentrations of boric acid revealed an overall sensitivity of all cloned aquaporins, suggesting that these aquaporins may be involved in the transport of boron. The same results have been also described in OsPIP1;3 and OsPIP2;6 (Mosa et al., 2016), in VvTnPIP1;4, VvTnPIP2;1, VvTnPIP2;3, VvTnTIP1;1 and VvTnTIP2;2 (Sabir et al., 2014).

## 5. Concluding remarks and Future perspectives

In conclusion, two *Q. suber* L. aquaporins, one PIP (PIP2;4) and one TIP (TIP2;1) were cloned and heterologously expressed in *S. cerevisiae*. Additionally, one mutated version of PIP2;4 was obtained during the cloning of PIP2;4, in which Threonine was replaced by a Serine at position 70. The two aquaporins were functional for water transport (QsTIP2;1 and QsPIP2;4A) while the mutant (QsPIP2;4B) was not. Increased susceptibility to boric acid and hydrogen peroxide suggest that these aquaporins may also be involved in transport of these atypical substrates. Additionally, contrary to what was expected, mercury chloride, a well-known aquaporin inhibitor, increased the water permeability in QsPIP2;4A expressing strain.

The results obtained provide an increase in the knowledge regarding plant aquaporins, in particular concerning *Quercus suber* L. and help to understand the effect of water stress (drought and flooding) in this economically important species. A point to be noted is that QsPIP2;4 and QsTIP2;1 were expressed in stems, and although one may speculate their role in tissues, expression studies directly in plants under stress factors need to be done. Yet, further analyses are needed in order to clearly understand the regulation and gating of these aquaporins, in particular, residues for putative regulatory sites as well as the role of Ar/R residues should also be addressed. A more fine-tuned approach, using site directed mutagenesis combined with 3D models of the pore region, may help to shed light on the relevant role of these specific residues.

## 6. References

- Almeida, A. De, Martins, A. P., Mosca, A. F., Wijma, H. J., Prista, C., Soveral, G., & Casini, A. (2016). Exploring the gating mechanisms of aquaporin-3: new clues for the design of inhibitors? *Molecular BioSystems*, *12*, 1564–1573. <https://doi.org/10.1039/c6mb00013d>
- Alves, C. (2014). *Studies on cork oak decline: an integrated approach. PhD Thesis.*
- Badaut, J., Lasbennes, F., Magistretti, P. J., & Regli, L. (2002). Aquaporins in Brain: Distribution, Physiology, and Pathophysiology. *Journal of Cerebral Blood Flow & Metabolism*, *22*, 367–378.
- Baranyi, J., & Roberts, T. A. (1994). A dynamic approach to predicting bacterial growth in food. *International Journal of Food Microbiology*, *24*, 277–294. [https://doi.org/10.1016/0168-1605\(94\)90157-0](https://doi.org/10.1016/0168-1605(94)90157-0)
- Berrahmouni, N., Regato, P., & Stein, C. (2007). Beyond Cork - a wealth of resources for people and nature, Lessons from the Mediterranean. *World Wide Fund for Nature*, 118.
- Besson, C. K., Lobo-do-Vale, R., Rodrigues, M. L., Almeida, P., Herd, A., Grant, O. M., ... Pereira, J. S. (2014). Cork oak physiological responses to manipulated water availability in a Mediterranean woodland. *Agricultural and Forest Meteorology*, *184*, 230–242. <https://doi.org/10.1016/j.agrformet.2013.10.004>
- Biela, A., Grote, K., Otto, B., Hoth, S., Hedrich, R., & Kaldenhoff, R. (1999). The Nicotiana tabacum plasma membrane aquaporin NtAQP1 is mercury-insensitive and permeable for glycerol. *Plant Journal*, *18*(5), 565–570. <https://doi.org/10.1046/j.1365-313X.1999.00474.x>
- Bienert, G. P., Møller, A. L. B., Kristiansen, K. A., Schulz, A., Møller, I. M., Schjoerring, J. K., ... C, D.-F. (2007). Specific Aquaporins Facilitate the Diffusion of Hydrogen Peroxide across Membranes \*. *The Journal of Biological Chemistry*, *282*(2), 1183–1192. <https://doi.org/10.1074/jbc.M603761200>
- Calamita, G. (2005). Aquaporins: highways for cells to recycle water with the outside world. *Biology of the Cell*, *97*, 351–353.
- Chaumont, F., Moshelion, M., & Daniels, M. J. (2005). Regulation of plant aquaporin activity. *Biology of the Cell*, *97*(10), 749–764. <https://doi.org/10.1042/BC20040133>
- Chaumont, F., & Tyerman, S. D. (2014). Aquaporins: Highly Regulated Channels Controlling Plant Water Relations. *Plant Physiology*, *164*(4), 1600–1618. <https://doi.org/10.1104/pp.113.233791>
- Crooks, G., Hon, G., Chandonia, J., & Brenner, S. (2004). WebLogo: a sequence logo generator. *Genome Research*, *14*, 1188–1190. <https://doi.org/10.1101/gr.849004.1>

- D.Schneider, T., & Stephens, R. M. (1990). Sequence logos: a new way to display consensus sequences. *Nucleic Acids Research*, *18*(20), 6097–6100.  
<https://doi.org/10.1006/mvre.1999.2194>
- D.Thompson, J., G.Higgins, D., & J.Gibson, T. (1994). CLUSTAL W: improving the sensitivity of progressive multiple sequence alignment through sequence weighting, position-specific gap penalties and weight matrix choice. *Nucleic Acids Research*, *22*(22), 4673–4680.  
<https://doi.org/10.1093/nar/22.22.4673>
- Daniels, M. J. (1996). Characterization of a New Vacuolar Membrane Aquaporin Sensitive to Mercury at a Unique Site. *The Plant Cell Online*, *8*(4), 587–599.  
<https://doi.org/10.1105/tpc.8.4.587>
- Duina, A. A., Miller, M. E., & Keeney, J. B. (2014). Budding yeast for budding geneticists: A primer on the *Saccharomyces cerevisiae* model system. *Genetics*, *197*(1), 33–48.  
<https://doi.org/10.1534/genetics.114.163188>
- Feldmann, H. (2010). *Yeast: Molecular and Cell Biology*. (H. Feldmann, Ed.) (2nd ed.). Wiley-Blackwell.
- Fischer, M., & Kaldenhoff, R. (2008). On the pH Regulation of Plant Aquaporins \*. *The Journal of Biological Chemistry*, *283*(49), 33889–33892. <https://doi.org/10.1074/jbc.M803865200>
- Forrest, K. L., & Bhawe, M. (2007). Major intrinsic proteins ( MIPs ) in plants : a complex gene family with major impacts on plant phenotype. *Functional and Integrative Genomics*, *7*, 263–289. <https://doi.org/10.1007/s10142-007-0049-4>
- Frick, A., Järvå, M., Ekvall, M., Uzdevinys, P., Nyblom, M., & Törnroth-Horsefield, S. (2013). Mercury increases water permeability of a plant aquaporin through a non-cysteine-related mechanism. *Biochemical Journal*, *454*(3), 491–499. <https://doi.org/10.1042/BJ20130377>
- Froger, A., Tallur, B., & Thomas, D. (1998). Prediction of functional residues in water channels and related proteins. *Protein Science*, *7*, 1458–1468.
- Fujiwara, T., Takano, J., Wada, M., Ludewig, U., & Schaaf, G. (2006). The Arabidopsis Major Intrinsic Protein NIP5 ; 1 Is Essential for Efficient Boron Uptake and Plant Development under Boron Limitation. *American Society of Plant Biologists*, *18*(June), 1498–1509.  
<https://doi.org/10.1105/tpc.106.041640.2>
- Gerbeau, P., Güçlü, J., Ripoche, P., & Maurel, C. (1999). Aquaporin Nt-TIPa can account for the high permeability of tobacco cell vacuolar membrane to small neutral solutes. *Plant Journal*, *18*(6), 577–587. <https://doi.org/10.1046/j.1365-313X.1999.00481.x>
- Gietz, R. D., & Schiestl, R. H. (2007). Quick and easy yeast transformation using the LiAc/SS carrier DNA/PEG method. *Nature Protocols*, *2*(1), 35–37.  
<https://doi.org/10.1038/nprot.2007.14>

- Gil, L. (2015). New cork-based materials and applications. *Materials*, 8(2), 625–637.  
<https://doi.org/10.3390/ma8020625>
- Giorgi, F., & Lionello, P. (2008). Climate change projections for the Mediterranean region. *Global and Planetary Change*, 63(2–3), 90–104.  
<https://doi.org/10.1016/j.gloplacha.2007.09.005>
- Hall, T. A. (1999). BioEdit: a user-friendly biological sequence alignment editor and analysis program for Windows 95/98/NT. *Nucleic Acids Symposium Series*, 41, 95–98.  
<https://doi.org/citeulike-article-id:691774>
- Han, R. Z., Wang, D., Chen, Y. H., Dong, L. K., & Fan, Y. L. (2017). Prediction of phosphorylation sites based on Krawtchouk image moments. *Genetics and Molecular Research*, 16(1), 1–9. <https://doi.org/10.1002/prot.25388>
- Heymann, J. B., & Engel, A. (2000). Structural Clues in the Sequences of the Aquaporins. *Journal of Molecular Biology*, 295, 1039–1053.
- Hofte, H., Hubbard, L., Reizer, J., Ludevid, D., Herman, E. M., & Chrispeels, M. J. (1992). Vegetative and Seed-Specific Forms of Tonoplast Intrinsic Protein in the Vacuolar Membrane of *Arabidopsis thaliana*. *Plant Physiology*, 99(2), 561–570.  
<https://doi.org/10.1104/pp.99.2.561>
- Hove, R. M., & Bhave, M. (2011). Plant aquaporins with non-aqua functions : deciphering the signature sequences. *Plant Molecular Biology*, 75, 413–430.  
<https://doi.org/10.1007/s11103-011-9737-5>
- Ikeda, M., Arai, M., Okuno, T., & Shimizu, T. (2003). TMPDB: a database of experimentally-characterized transmembrane topologies. *Nucleic Acids Research*, 31(1), 406–409.  
<https://doi.org/10.1093/nar/gkg018>
- Ines, O. (2008). Functional analysis of PIP2 aquaporins in *Arabidopsis thaliana*. *Thesis*.
- Ishikawa, F., Suga, S., Uemura, T., Sato, M. H., & Maeshima, M. (2005). Novel type aquaporin SIPs are mainly localized to the ER membrane and show cell-specific expression in *Arabidopsis thaliana*. *FEBS Letters*, 579(25), 5814–5820.  
<https://doi.org/10.1016/j.febslet.2005.09.076>
- Javot, H., & Maurel, C. (2002). The role of aquaporins in root water uptake. *Annals of Botany*, 90(3), 301–313. <https://doi.org/10.1093/aob/mcf199>
- Kalam, A., Yoshikawa, N., Ishikawa, T., Sawa, Y., & Shibata, H. (2012). Substitution of a single amino acid residue in the aromatic / arginine selectivity filter alters the transport profiles of tonoplast aquaporin homologs. *BBA - Biomembranes*, 1818(1), 1–11.  
<https://doi.org/10.1016/j.bbamem.2011.09.014>
- Katsuhara, M., Sasano, S., Horie, T., Matsumoto, T., Rhee, J., & Shibasaka, M. (2014).

- Functional and molecular characteristics of rice and barley NIP aquaporins transporting water, hydrogen peroxide and arsenite. *Plant Biotechnology*, 31, 213–219.  
<https://doi.org/10.5511/plantbiotechnology.14.0421a>
- Kirscht, A., Survery, S., Kjellbom, P., & Johanson, U. (2016). Increased Permeability of the Aquaporin So PIP2; 1 by Mercury and Mutations in Loop A. *Frontiers in Plant Science*, 7(August), 1249. <https://doi.org/10.3389/fpls.2016.01249>
- Kjellbom, P., Larsson, C., Johansson, I., Karlsson, M., & Johanson, U. (1999). Aquaporins and water homeostasis in plants. *Trends in Plant Science*, 1385(99).
- Krogh, A., Larsson, B., Von Heijne, G., & Sonnhammer, E. L. L. (2001). Predicting transmembrane protein topology with a hidden Markov model: Application to complete genomes. *Journal of Molecular Biology*, 305(3), 567–580.  
<https://doi.org/10.1006/jmbi.2000.4315>
- Kruse, E., Uehlein, N., & Kaldenhoff, R. (2006). Protein family review The aquaporins.  
<https://doi.org/10.1186/gb-2006-7-2-206>
- Kumar, S., Stecher, G., Li, M., Knyaz, C., & Tamura, K. (2018). MEGA X: Molecular evolutionary genetics analysis across computing platforms. *Molecular Biology and Evolution*, 35(6), 1547–1549. <https://doi.org/10.1093/molbev/msy096>
- Laloux, T., Junqueira, B., Maistriaux, L. C., Ahmed, J., Jurkiewicz, A., & Chaumont, F. (2018). Plant and mammal aquaporins: Same but different. *International Journal of Molecular Sciences*, 19(2). <https://doi.org/10.3390/ijms19020521>
- Leitão, L., Prista, C., Loureiro-Dias, M. C., Moura, T. F., & Soveral, G. (2014). The grapevine tonoplast aquaporin TIP2;1 is a pressure gated water channel. *Biochemical and Biophysical Research Communications*, 450(1), 289–294.  
<https://doi.org/10.1016/j.bbrc.2014.05.121>
- Leitão, L., Prista, C., Moura, T. F., Loureiro-Dias, M. C., & Soveral, G. (2012). Grapevine aquaporins: Gating of a tonoplast intrinsic protein (TIP2;1) by cytosolic pH. *PLoS ONE*, 7(3). <https://doi.org/10.1371/journal.pone.0033219>
- Li, G., Santoni, V., & Maurel, C. (2014). Plant aquaporins: Roles in plant physiology. *Biochimica et Biophysica Acta - General Subjects*, 1840(5), 1574–1582.  
<https://doi.org/10.1016/j.bbagen.2013.11.004>
- Liu, L.-H. (2003). Urea Transport by Nitrogen-Regulated Tonoplast Intrinsic Proteins in Arabidopsis. *Plant Physiology*, 133(3), 1220–1228. <https://doi.org/10.1104/pp.103.027409>
- Maurel, C. (2007). Plant aquaporins: Novel functions and regulation properties. *FEBS Letters*, 581, 2227–2236. <https://doi.org/10.1016/j.febslet.2007.03.021>
- Maurel, C., Boursiac, Y., Luu, D.-T., Santoni, V., Shahzad, Z., & Verdoucq, L. (2015).

- Aquaporins in Plants. *Physiological Reviews*, 95(4), 1321–1358.  
<https://doi.org/10.1152/physrev.00008.2015>
- Maurel, C., Reizer, J., Schroeder, J. I., & Chrispeels, M. J. (1993). The vacuolar membrane protein. *Embo*, 12(6), 2241–2247.
- Maurel, C., Végétales, S., & Terrasse, A. De. (1997). Aquaporins and Water Permeability of Plant Membranes. *Annual Review of Plant Biology and Plant Molecular Biology*, 48, 399–429.
- Maurel, C., Verdoucq, L., & Luu, D. (2008). Plant Aquaporins : Membrane Channels with Multiple Integrated Functions. *Annual Review of Plant Biology*, 59, 595–624.  
<https://doi.org/10.1146/annurev.arplant.59.032607.092734>
- Mbonyi, K., Aelst, L. Van, Arguelles, J. C., Jans, A. W. H., & Thevelein, J. M. (1990). Glucose-Induced Hyperaccumulation of Cyclic AMP and Defective Glucose Repression in Yeast Strains with Reduced Activity of Cyclic AMP-Dependent Protein Kinase, 10(9), 1–115.
- Modesto, I. (2012). *Assessing adaptive genetic variation in cork oak expressed genes*. Faculdade.
- Mosa, K. A., Kumar, K., Chhikara, S., Musante, C., & White, J. C. (2016). Enhanced Boron Tolerance in Plants Mediated by Bidirectional Transport Through Plasma Membrane Intrinsic Proteins. *Nature Publishing Group*, (September 2015), 1–14.  
<https://doi.org/10.1038/srep21640>
- Mósca, A., Andreia De, A., Darren, W., Ana P, M., Farzana, S., Stefano, L., ... Graça, S. (2018). Molecular Basis of Aquaporin-7 Permeability Regulation by pH. *Cells*, 7(207), 1–20.  
<https://doi.org/10.3390/cells7110207>
- Moshelion, M., Moran, N., & Chaumont, F. (2004). Dynamic changes in the osmotic water permeability of protoplast plasma membrane. *Plant Physiology*, 135(4), 2301–2317.  
<https://doi.org/10.1104/pp.104.043000.1>
- Ozu, M., Dorr, R. A., Gutiérrez, F., Teresa Politi, M., & Toriano, R. (2013). Human AQP1 is a constitutively open channel that closes by a membrane-tension-mediated mechanism. *Biophysical Journal*, 104(1), 85–95. <https://doi.org/10.1016/j.bpj.2012.11.3818>
- Pereira-Leal, J. B., Abreu, I. A., Alabaça, C. S., Almeida, M. H., Almeida, P., Almeida, T., ... Ricardo, C. P. P. (2014). A comprehensive assessment of the transcriptome of Cork oak (*Quercus suber*) through EST sequencing. *BMC Genomics*, 15(1), 1–14.  
<https://doi.org/10.1186/1471-2164-15-371>
- Plant, T., April, C., Becker, D., Moshelion, M., Becker, D., Biela, A., ... Otto, B. (2002). Plasma Membrane Aquaporins in the Motor Cells of *Samanea saman* : Diurnal and Circadian Regulation Plasma Membrane Aquaporins in the Motor Cells of *Samanea saman* : Diurnal

- and Circadian Regulation. *The Plant Cell*, 14(March), 727–739.  
<https://doi.org/10.1105/tpc.010351.these>
- Rodrigues, C., Mósca, A. F., Martins, A. P., Nobre, T., Prista, C., Antunes, F., ... Soveral, G. (2016). Rat aquaporin-5 is pH-gated induced by phosphorylation and is implicated in oxidative stress. *International Journal of Molecular Sciences*, 17(12), 1–19.  
<https://doi.org/10.3390/ijms17122090>
- Sabir, F., Leandro, M. J., Martins, A. P., Loureiro-dias, M. C., Moura, T. F., Soveral, G., & Prista, C. (2014). Exploring Three PIPs and Three TIPs of Grapevine for Transport of Water and Atypical Substrates through Heterologous Expression in aqy-null Yeast. *PLoS ONE*, 9(8).  
<https://doi.org/10.1371/journal.pone.0102087>
- Schaffner, A. R. (1998). Review Aquaporin function , structure , and expression : are there more surprises to surface in water relations ? *Planta*, 204, 131–139.
- Shapiguzov, A. Y. (2004). Aquaporins : Structure , Systematics , and Regulatory Features. *Russian Journal of Plant Physiology*, 51(1), 142–152.
- Sonnhammer, E. L. L., Heijne, G., & Krogh, A. (1998). A hidden Markov model for predicting transmembrane helices in protein sequences. *Proceedings of the Sixth International Conference on Intelligent Systems for Molecular Biology*, 175–182. Retrieved from <papers://4b986d00-906f-493f-a74b-71e29d82b719/Paper/p6291>
- Soveral, G., Madeira, A., Loureiro-Dias, M. C., & Moura, T. F. (2008). Membrane tension regulates water transport in yeast. *Biochimica et Biophysica Acta - Biomembranes*, 1778(11), 2573–2579. <https://doi.org/10.1016/j.bbamem.2008.07.018>
- Soveral, G., Prista, C., Moura, T. F., & Loureiro-Dias, M. C. (2011). Yeast water channels: an overview of orthodox aquaporins. *Biology of the Cell*, 103(1), 35–54.  
<https://doi.org/10.1042/BC20100102>
- Soveral, G., Trincão, J., & Moura, T. F. (2011). Aquaporins: membrane channels for water transport. *Canal BQ*, 8(July), 36–43. <https://doi.org/10.1016/B978-0-12-378630-2.00055-4>
- Surový, P., & Ribeiro, N. (2008). *Inventário nacional de mortalidade de sobreiro na fotografia aérea digital de 2004/2006*.
- Taiz, L., & Zeiger, E. (2002). *Plant Physiology* (3rd ed.). Sinauer Associates.
- Takata, K., Matsuzaki, T., & Tajika, Y. (2004). Aquaporins: Water channel proteins of the cell membrane. *Progress in Histochemistry and Cytochemistry*, 39(1), 1–83.  
<https://doi.org/10.1016/j.proghi.2004.03.001>
- Törnroth-Horsefield, S., Wang, Y., Hedfalk, K., Johanson, U., Karlsson, M., Tajkhorshid, E., ... Kjellbom, P. (2006). Structural mechanism of plant aquaporin gating. *Nature*, 439(7077), 688–694. <https://doi.org/10.1038/nature04316>

- Tournaire-Roux C, Sutka M, Javot H, Gout E, G. P. et al. (2003). Cytosolic pH regulates root water transport during anoxic stress through gating of aquaporins. *Nature*, 425, 393–397.
- Uehlein, N., Lovisolo, C., Siefritz, F., & Kaldenhoff, R. (2003). The tobacco aquaporin NtAQP1 is a membrane CO<sub>2</sub> pore with physiological functions. *Nature Publishing Group*, 425(OCTOBER), 734–737.
- Vajpai, M., Mukherjee, M., & Sankararamakrishnan, R. (2018). Cooperativity in Plant Plasma Membrane Intrinsic Proteins (PIPs): Mechanism of Increased Water Transport in Maize PIP1 Channels in Hetero-tetramers. *Scientific Reports*, 8(1), 1–17.  
<https://doi.org/10.1038/s41598-018-30257-4>
- Verdoucq, L., Rodrigues, O., Martinière, A., Luu, D. T., & Maurel, C. (2014). Plant aquaporins on the move : reversible phosphorylation , lateral motion and cycling. *Current Opinion in Plant Biology*, 22, 101–107. <https://doi.org/10.1016/j.pbi.2014.09.011>
- Wallace, I. S., & Roberts, D. M. (2004). Homology Modeling of Representative Subfamilies of Arabidopsis Major Intrinsic Proteins . Classification Based on the Aromatic / Arginine Selectivity Filter 1[w]. *Plant Physiology*, 135(June), 1059–1068.  
<https://doi.org/10.1104/pp.103.033415.small>
- Yang, F., Kawedia, J. D., & Menon, A. G. (2003). Cyclic AMP regulates aquaporin 5 expression at both transcriptional and post-transcriptional levels through a protein kinase A pathway. *Journal of Biological Chemistry*, 278(34), 32173–32180.  
<https://doi.org/10.1074/jbc.M305149200>

# Annexes

## Annex I. Cloning and heterologous expression of QsTIP2;1 and QsPIP2;4

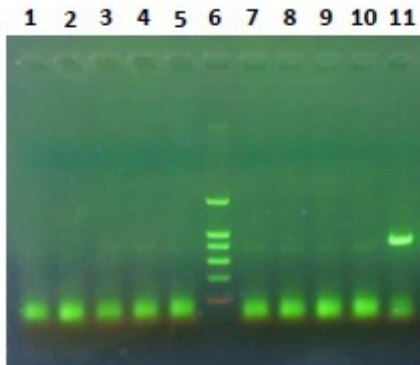


Figure 0.1 - Gradient PCR with A2 cDNA. From lane 1 to lane 10 temperature rises from 50°C to 60°C and then from 55°C to 65° in the second cycle. Lane 6 is ladder and lane 11 is positive control

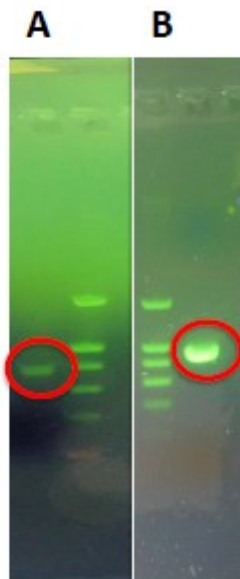


Figure 0.2 - Result of gel-purification of TIP2;1 aquaporin (A) and PIP2;4 (B).

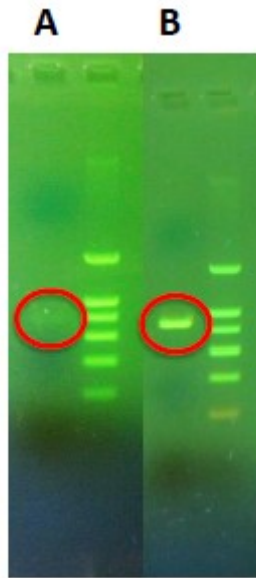


Figure 0.3 - Result of purification after digestion of TIP2;1 (A) and PIP2;4 (B)

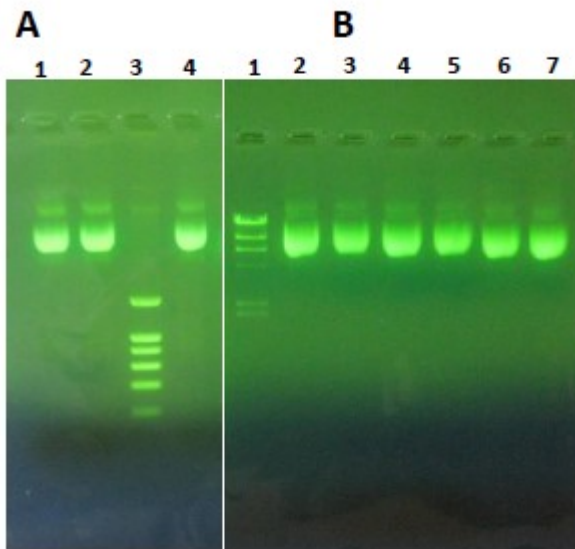


Figure 0.4 - Plasmid extraction of transformants cloned with TIP 2;1 (A) and PIP2;4 (B). (A): lane 1 – A2; lane 2 – B2; lane 3 – ladder and lane 4 – F1. (B): lane 1 – lambda hind III; lane 2 – A1; lane 3 – A2; lane 4 – B2; lane 5 – B3; lane 6 – D3 and lane 7 – E.

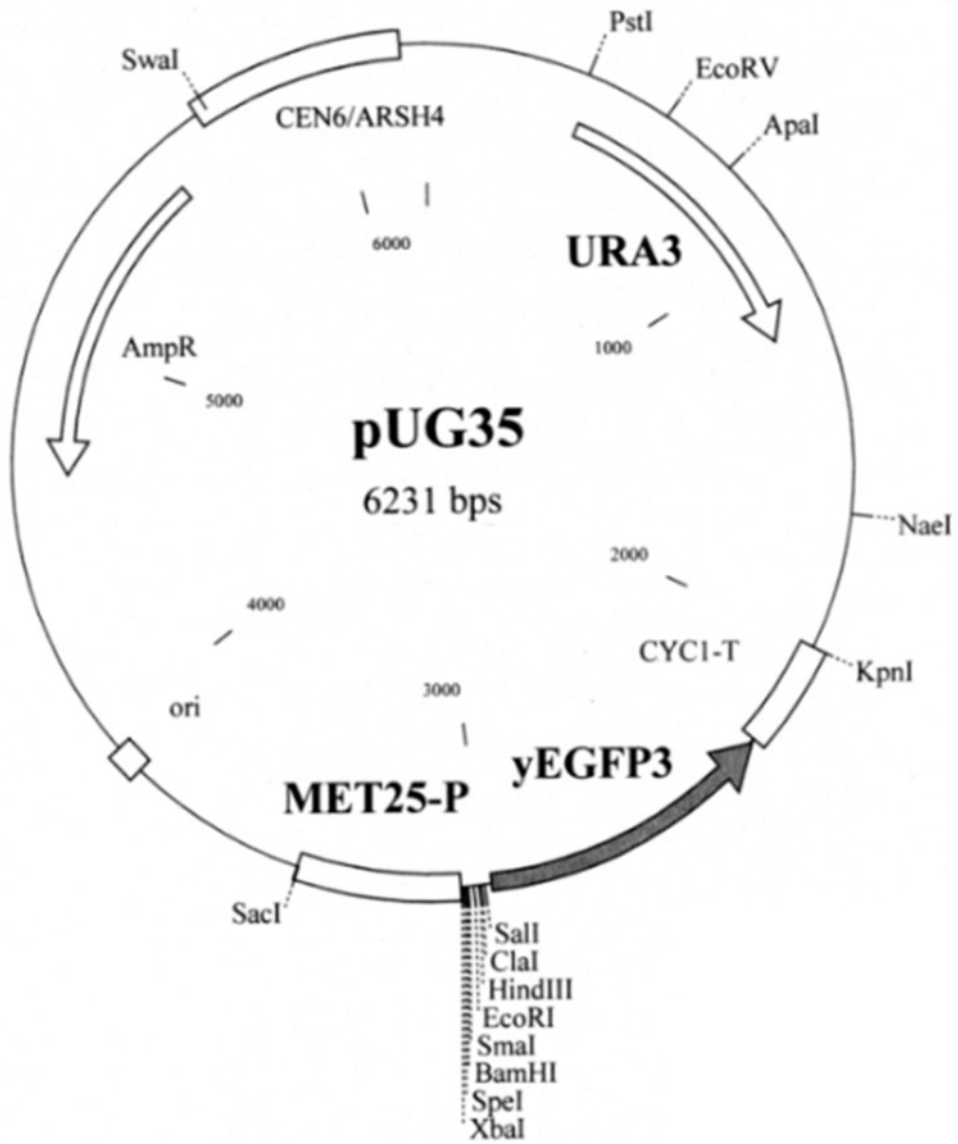


Figure 0.5 - pUG35 plasmid map.